SUBAXOLEMMAL FILAMENTOUS NETWORK IN THE GIANT NERVE FIBER OF THE SQUID (*LOLIGO PEALEI* L.) AND ITS POSSIBLE ROLE IN EXCITABILITY

J. METUZALS and I. TASAKI

From the Electron Microscopy Unit, Department of Anatomy, Faculty of Medicine, University of Ottawa, Canada, and the Marine Biological Laboratory, Woods Hole, Massachusetts 02543. Dr. Metuzals' present address is the Max-Planck-Institut für Biophysikalische Chemie, Göttingen, West Germany, and Dr. Tasaki's present address is the Laboratory of Neurobiology, National Institute of Mental Health, Bethesda, Maryland 20014

ABSTRACT

A new technique utilizing the squid giant nerve fiber has been developed which permits direct examination of the inner face of the axolemma by scanning electron microscopy. The axoplasm was removed sequentially in a 15-mm long segment of the fiber by intracellular perfusion with a solution of KF, KCl, Ca^{++}-containing seawater, or with pronase. The action potential of the fibers was monitored during these treatments. After brief prefixation in 1% paraformaldehyde and 1% glutaraldehyde, the perfused segment was opened by a longitudinal cut with a razor blade. The overall view of the opened perfusion zone could be related to information on the detailed morphology of the cytoplasmic face of the axolemma and the ectoplasm. The results obtained by scanning electron microscopy were further substantiated by transmission electron microscopy of thin sections. In addition, living axons were studied with polarized light during axoplasm removal, and the identification of actin by heavy meromyosin labeling and sodium dodecyl sulfate (SDS)-polyacrylamide gel electrophoresis was accomplished. These observations demonstrate that a three-dimensional network of interwoven filaments, consisting partly of an actinlike protein, is firmly attached to the axolemma. The axoplasmic face of fibers in which the filaments have been removed partially after perfusion with pronase displays smooth membranous blebs and large profiles which appose the axolemma. In fibers where the excitability has been suppressed by pronase perfusion, approximately one-third of the inner face of the axolemma in the perfusion zone is free of filaments. It is hypothesized that the attachment of axoplasm filaments to the axolemma may have a role in the maintenance of the normal morphology of the axolemma, and, thus, in some aspect of excitability.

KEY WORDS squid giant nerve fiber · subaxolemmal filamentous network · actin · excitability

Investigation of the relationships between the axoplasm and the axolemma has been limited by the inaccessibility of the inner surface of the axolemma to direct examination. We report in this paper a strategem for a direct and selective exploration of the cytoplasmic surface of the axo-

lemma by combining scanning electron microscopy with intracellular perfusion and electrical recording of the squid giant nerve fiber. With such a technique, the inner surface components of the axolemma are fully accessible and, furthermore, adequate quantities of uncontaminated samples of axoplasm are easily obtained for chemical analysis.

Previously, a lattice structure has been observed in the axoplasm of the squid giant nerve fiber (27). Numerous ~70-Å wide filaments of the ectoplasm could be identified in association with the axolemma (27, 26). Noteworthy in this connection is the demonstration of transient changes in the optical properties of the ectoplasm during action potentials (60, 45).

In the past the plasma membrane was considered to be an autonomous lipid bilayer with few interspersed proteins. It is becoming increasingly apparent that the plasma membrane is in fact a complex organelle, coupled to various cytoplasmic structures, and under strict and coordinated cytoplasmic control (50, 34). We have examined the effects of sequential removal of the ectoplasm components on the structure and excitability of the giant nerve fiber. On the basis of our results, we hypothesize that the subaxolemmal filamentous network, which is partly composed of actin-like protein, may have a role in the maintenance of the normal morphology of the axolemma and, thus, probably in some aspect of excitability.[1]

MATERIALS AND METHODS

All the experiments and observations were made on the giant nerve fiber of the squid (*Loligo pealei* L.) obtained at the Marine Biological Laboratory (Woods Hole, Mass.) during the summers of 1972–1976. The animals used had spent no more than a few hours in laboratory tanks containing running seawater. Dissection of the dorsal giant nerve fiber was performed under running seawater on a dissecting table illuminated from below through a glass window.

Solutions

The salt solutions routinely used had the following compositions. Artificial seawater (ASW) for external use: 423 mM NaCl, 9 mM KCl, 23 mM $MgCl_2$, 25 mM $MgSO_4$, 10 mM $CaCl_2$, and 5 mM Tris (pH 7.9–8.1). The ASW used for solubilization of the fixatives contained 15 mM $NaHCO_3$ (pH adjusted to 7.2–7.4) instead of Tris. The standard salt solution (SSS) contained 0.05 M KCl, 0.005 M $MgCl_2$, 0.006 M phosphate buffer (pH 7.0). Pronase (Calbiochem, San Diego, Calif.) was dissolved in KF-phosphate solution. The composition of the KF-phosphate solution was 400 meq/liter K-ion, 350 meq/liter F-ion, phosphate (potassium salt) buffer adjusted at pH 7.2–7.4, and glycerol (4% vol/vol).

Intracellular Perfusion of the Axon

The technique for removal of axoplasm from the squid giant nerve fiber and subsequent intracellular perfusion of the axon has been described in detail elsewhere (59). The major portion of small nerve fibers and other adherent tissues surrounding the giant fiber were removed under a dissecting microscope. An excised nerve fiber, ~35 mm in length and ligated at each end with a thread, was placed in a shallow pool of ASW in a chamber made of transparent Lucite. Under a dissecting microscope, a glass cannula was inserted into each end of the giant nerve fiber. The micro-cannula introduced into the proximal end of the fiber was 300 μm in outside diameter. The tip of this cannula was beveled and ground in the form of a chisel to enable it to cut the solid portion of the axoplasm. As the micro-cannula was advanced along the axis of the nerve fiber with the aid of a micromanipulator, the endoplasm of the axon was sucked into the cannula by applying negative pressure through polyethylene tubing connected to the blunt end of the micro-cannula. Afterwards, a 10–20-mm long portion of the axon was intracellularly perfused with various solutions for variable periods of time to remove the axoplasm partially or completely. A flow rate of the internal perfusion fluid was maintained at 20–30 μl/min. During the entire period of the experiment, the excitability of the nerve fiber was monitored by means of a stimulator and a cathode-ray oscilloscope connected to metal electrodes on the surface of the fiber and to an intra-axonal electrode placed in the perfusion zone. After the perfusion, an air bubble was introduced into the perfusion zone, and the ends of fiber were sealed by coagulating the axoplasm outside the perfusion zone with a heated needle.

Scanning Electron Microscopy

For scanning electron microscopy, special stubs were prepared from stainless steel. The top of the stubs was buffed to a mirrorlike finish. A shallow groove was filed around the stub near the top. A 3-cm long fiber, filled with air in the perfusion zone, was stretched across the buffed top of the stub under the dissecting microscope. The overhanging ends of the fiber were tied to the stub by a loop of 100-μm enameled silver wire which was tightened in the groove around the stub. After 15 min of prefixation in 1% paraformaldehyde and 1% glutaraldehyde dissolved in ASW, the wall of the perfused segment was cut longitudinally with the sharp tip of a broken razor blade. Then the portion of the wall above

[1] The results of this work were presented at the First International Congress on Cell Biology, Boston, 1976 (30) and at the Annual Meeting of the Marine Biological Laboratory, Woods Hole, 1974 (29).

the cut was removed, and the inner face of the giant fiber in the perfusion zone was exposed. During cutting, fixation fluid was repeatedly poured on the fiber with a pipette. The stub with the fiber was always kept submerged in the corresponding fluids.

After prefixation, the opened fibers were fixed for 1–2 h in the same fixative, followed by rinsing in three changes of ASW, 5 min each change. Finally, the specimens were fixed in 1% osmium tetroxide dissolved in 0.5 M sodium cacodylate buffer, pH 7.4, of the same osmolality as the ASW (1,010 mosmol/liter). All stages of fixation, rinsing, and dehydration were carried out at room temperature.

After fixation, samples were dehydrated through a graded series of ethanol solutions (25, 50, 75, 80, 90, and 96%) to 100%, 1–5 min each step. From here the preparations were carried through a graded series of amyl acetate in alcohol up to 100% amyl acetate. (In about half of the preparations, the treatment with amyl acetate was omitted.) Then the specimens were transferred into liquid CO_2 in a critical-point drying apparatus (Samdri pvt-3, Tousimis Research Corp., Rockville, Md.). The resulting dry specimens were coated with gold-palladium. During all the preparative steps and the actual observation in the scanning electron microscope, the fiber remained attached to the same stub.

A JEOL JSM-35 U scanning electron microscope with a eucentric goniometric meter, operated at 20 kV, was used in all the studies.

Negative Staining, Heavy Meromyosin Treatment and Thin Sectioning

In each series of experiments, axoplasm was extruded, usually from two to four dissected fibers, onto parafilm and washed into a homogenization tube with a few drops of SSS. About 50–100 μl of axoplasm was diluted into 0.5 or 2 ml of the SSS and homogenized by 15 strokes of a Teflon pestle.

The standard procedure for negative staining was as follows: A drop of diluted axoplasm was placed on a copper grid coated with Formvar and carbon, fixed for 1 min with 1% formalin dissolved in the SSS, washed afterwards with the SSS, and rinsed with 0.1 M KCl. Staining was carried out for 1–3 min with 1% uranyl acetate at pH 4.4, and excess uranyl solution was removed with small pieces of filter paper. Fixation with formalin was ofen omitted.

Myosin from rabbit muscle was prepared according to Mommaerts and Parrish (31) and was subsequently treated with trypsin as described by Lowey and Cohen (23) to obtain heavy meromyosin (HMM). HMM in 25% glycerol was always diluted to 400 μg/ml in the SSS used to dilute the axoplasm.

HMM-labeling was carried out according to the following procedure: A drop of diluted axoplasm was placed on a carbon-coated grid, and the excess was rinsed off. A few drops of HMM were then placed on the grid for 5 min, followed by fixation with 1% formalin, rinsing with 0.1 M KCl, and negative staining. Fixation in 1% formalin was often omitted. In control experiments, HMM was omitted or the HMM-axoplasm suspension was incubated in the presence of 10 mM ATP for 5 min.

The treatment of glycerinated whole giant nerve fibers with HMM was carried out as follows (19): Dissected fibers were stored in 50% glycerol at −20°C for several weeks. The concentration of glycerol was decreased stepwise over a period of 24 h until the fibers were in pure SSS. Subsequent treatment with HMM dissolved in SSS was carried out for 12 h at 4°C. Fibers treated with HMM were washed in two changes of 0.1 M KCl, and then fixed, dehydrated, and embedded according to standard procedures. In control experiments, HMM was omitted or incubation was carried out with HMM in SSS containing 10 mM ATP.

Transmission Electron Microscopy

Standard procedures were used for transmission electron microscopy of thin sections. The fixation was carried out by direct immersion of the dissected fiber, still surrounded by a connective tissue layer and blood vessels, into the fixative. Therefore, the quality of fixation, especially of intact fibers, was lower than in vertebrates fixed by perfusion. The intact and the perfused fibers were first fixed for 1–2 h in 1% paraformaldehyde and 1% glutaraldehyde dissolved in ASW, pH 7.2–7.4. After washing in three changes of ASW for 5 min, the fibers were postfixed for 15 min in 1% osmium tetroxide dissolved in 0.51 M sodium cacodylate buffer (pH 7.4) of the same osmolality as the ASW (1,010 mosmol/liter) (26). Intact and perfused fibers were fixed also directly in 1% osmium tetroxide for 1–2 h without prior prefixation in aldehydes. The fibers were then washed briefly in distilled water, dehydrated (see section on Scanning Electron Microscopy), and embedded in Vestopal W (M. Jaeger, Geneva, Switzerland). All the stages of fixation, rinsing, and dehydration were carried out at room temperature. Ultrathin sections were cut on an LKB Ultrotome (LKB Instruments, Inc., Rockville, Md.) with glass knives. The sections were mounted on copper grids coated with Formvar and carbon and double stained with saturated uranyl acetate in ethanol followed by Reynolds' lead citrate (42).

All specimens on the grids were examined in an Elmiskop 1 A, Elmiskop 101, or JEM-100 B electron microscope equipped with a cold stage and operated at 80 kV with double condenser illumination and a 30-μm, thin foil objective aperture.

SDS-Polyacrylamide Gel Electrophoresis

Polyacrylamide gel electrophoresis of axoplasmic polypeptides in the presence of SDS was carried out in the discontinuous system of Laemmli (21), and the gels were fixed and stained as described by Fairbanks et al.

(12). The Shandon disc electrophoresis apparatus (Shandon Southern Instruments, Inc., Sewickley, Pa.) was used. The diameter of the gels was 0.5 cm, the stacking gel being 1 cm in length and the separating gel, 8 cm in length. The gels were run at a constant voltage of 50 V and the runs were terminated when the leading sample buffer/gel buffer interface had travelled through 7 cm of the separating gel. The relative electrophoretic mobility of the fractionated polypeptides and their molecular weights were determined as described by Weber and Osborn (64). Polypeptide standards were run in parallel with sample gels, and a standard curve was constructed utilizing 14 polypeptides with mol wt ranging from 13,700 (ribonuclease A) to 215,000 (rabbit skeletal muscle myosin). In most instances the running gel consisted of 10% polyacrylamide, but 5% polyacrylamide gels were used in some instances to improve characterization of high molecular weight components. Acetone powder was prepared from rabbit skeletal muscle by the procedure of Straub as described by Szent-Györgyi (57). Actin was extracted and purified by the procedure of Spudich and Watt (54).

For studies on freshly extruded axoplasm from squid giant fibers, the axoplasm was placed directly into electrophoresis sample buffer, which had the following composition: 2% SDS; 5% β-mercaptoethanol (β-MSH); 10% glycerol; 1 mM phenylmethyl sulfonylfluoride, a protease inhibitor; and 62.5 mM Tris-HCl, pH 6.8. The axoplasm was suspended by means of a Teflon-glass homogenizer, incubated at 45°C for 1 h and then heated at 100°C for 4 min. The solubilized material was then dialyzed against sample buffer. In some experiments, lipids were extracted to rule out the possibility that some of the stained bands on the gels contained lipid. These samples gave gel patterns identical to those obtained with untreated axoplasm.

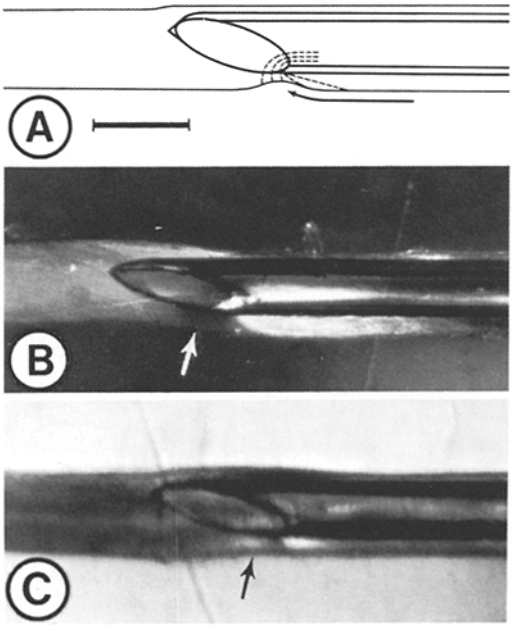

FIGURE 1 (*A*) Schematic representation of the arrangement of filaments (shown by the broken lines) in a fanlike pattern revealed by rotating both the polarizer and analyzer relative to the long axis of the nerve fiber. The arrow indicates the direction of displacement of the axon surface caused by suction. (*B* and *C*) Photographs of squid giant nerve fibers into which a glass micro-cannula is inserted. During the process of insertion of the cannula, a fanlike structure is seen near the rear portion of the orifice of the cannula (cf. Fig. 1*A*). (*B*) The giant fiber is placed between a polarizer and an analyzer which are approximately perpendicular to each other. The polarizing axis of the polarizer is roughly parallel to the long axis of the cannula. Under transillumination, the fanlike structure appears as a dark zone (indicated by the arrow) followed by a very bright zone. (*C*) Similar to Fig. 1*B*, except that the polarizing axes of the polarizer and analyzer are rotated slightly to show the orientation of the fibrous material giving rise to the birefringence. The fanlike structure (arrow) is lighter than the dark axoplasm. Bar, 0.5 mm. × 25.

RESULTS

Observations of the Axoplasm during Insertion of a Micro-Cannula into Living Nerve Fibers

The properties of the axon have been studied in living nerve fibers by the technique of axoplasm removal by a micro-cannula as described in Materials and Methods. A major portion of the axoplasm, predominantly the endoplasm, can be removed from the giant nerve fiber without suppressing its excitability. The glass micro-cannula used for this purpose has a sharp cutting edge, as illustrated in Fig. 1. The sharp, beveled tip of the cannula is designed to pierce the axoplasm by disrupting the intra-axonal network of fibrous proteins. Except in the case of large fibers with nearly fluid axoplasm, introduction of a micro-cannula with a blunt tip into the fiber interior is practically impossible.

As the axoplasm is drawn into the micro-cannula by suction, a characteristic fanlike pattern of fibrous material can be observed at the rear portion of the orifice of the micro-cannula. Depending on the conditions of illumination with unpolarized light, this pattern may appear bright or dark. By varying illumination, it is found that the fibrous material which forms this fanlike pattern extends from the surface of the axon into the

lumen of the micro-cannula.

In some nerve fibers, strong suction produces a displacement of the axon surface towards the orifice of the micro-cannula at the site or behind the attachment of the fanlike structure (Fig. 1). Such a displacement of the axon surface frequently brings about local injury of the fiber, resulting in a loss of its ability to conduct action potentials. In large nerve fibers (400–700 μm in diameter), it is relatively easy to advance the micro-cannula in the axoplasm without injuring the nerve fiber. In fibers kept at ~6°C for 2–3 h, the fanlike pattern is not so conspicuous as in freshly excised, relatively small fibers.

The fanlike pattern in the axoplasm has been examined by inserting two polarizing filters in the light path, a polarizer between the light source and the nerve fiber, and an analyzer between the fiber and the objective of the dissecting microscope. Under the cross-polar conditions, it is found that the fanlike structure is highly birefringent. Through rotation of the polarizing filters, it can be shown that the birefringent material within the fanlike structure extends obliquely from the surface of the fiber into the lumen of the micro-cannula (Fig. 1 *B* and *C*). From these observations, it is concluded that the fanlike pattern is formed by the filamentous material in the ectoplasm. The reason why the fanlike pattern appears predominantly near the axon surface around the trailing edge of the orifice of the micro-cannula is likely to be that the filaments at the leading edge of the orifice are readily displaced or cut by the sharp edge.

Scanning Electron Microscopy and Electrophysiology of Intracellularly Perfused Fibers

In this series of investigations, it was essential to develop a new, reliable technique of exposing the inner (i.e. axoplasmic) surface of the axolemma to electron beam. The technique developed for this purpose was to fasten a 15-mm long segment of an internally perfused fiber securely to a stub. After a brief prefixation, the upper half of the nerve fiber was resected (see Materials and Methods). This technique prevented an inadvertent interchange of the exposed inner surface of the perfusion zone with the outer connective tissue surface of the nerve fiber (Fig. 2).

PERFUSION WITH KF-PHOSPHATE: The inner surface of the ectoplasm of fibers perfused intracellularly with KF-phosphate solution for 50 min (see Materials and Methods) shows threadlike elements interwoven in a regular cross-lattice pattern (Fig. 3*A*). The thicker threads of the cross-lattice measure 0.3 μm and the finer ones are 0.1 μm in diameter. The cross-lattice pattern is oriented symmetrically about the long axis of the axon, and the angle between the two main components of the lattice is ~45°. In other portions of the same preparation, instead of a cross-lattice pattern, a matlike network assembly of 0.1-μm wide threads predominates. The components of this network appear wavy and curved. Points where thicker threads branch into finer components can be seen (arrow, Fig. 3*B*). The electrophysiological properties (the amplitude and the duration of the action potential, the conduction velocity, the threshold, etc.) remain perfectly normal during the entire period of perfusion with an isotonic KF-phosphate solution (59).

A cross-lattice pattern cannot be seen in fibers from which the endoplasm has been removed by suction only. Instead, the inner cytoplasmic face of such preparations displays predominantly smooth surfaces and irregular elevations.

PRONASE PERFUSION WITH RETAINED EXCITABILITY: Fibers perfused with pronase (0.1 mg/ml) in KF-phosphate for 10 min do not show any changes in their electrophysiological properties (see Fig. 9 A). (Pronase digests almost any protein virtually to free amino acids.) A continuous three-dimensional network consisting of threadlike elements extends on the inner side of the axolemma (Fig. 4). The threads are defined much more distinctly than in fibers perfused with KF-phosphate without pronase. The diameter of the threads varies over a wide range: from ~300 Å up to 0.3 μm. The threads appear curved and wavy and are interwoven in a network covering the inner face of the axolemma as a dense matrix. In micrographs taken at higher resolution, the beaded and the coiled appearance of the threads and their assembly into thicker threads can be seen clearly (asterisk, Fig. 4*B*). Furthermore, the continuous network character of this structure is evident (arrows, Fig. 4*B*). The three-dimensional character of the ectoplasmic network adjoining the axolemma is better appreciated in stereo-pair micrographs (Fig. 4*C*). In these micrographs, small areas can be identified as smooth inner face of the axolemma free of filaments.

Compared with the appearance of the ectoplasm of fibers internally perfused with KF-phos-

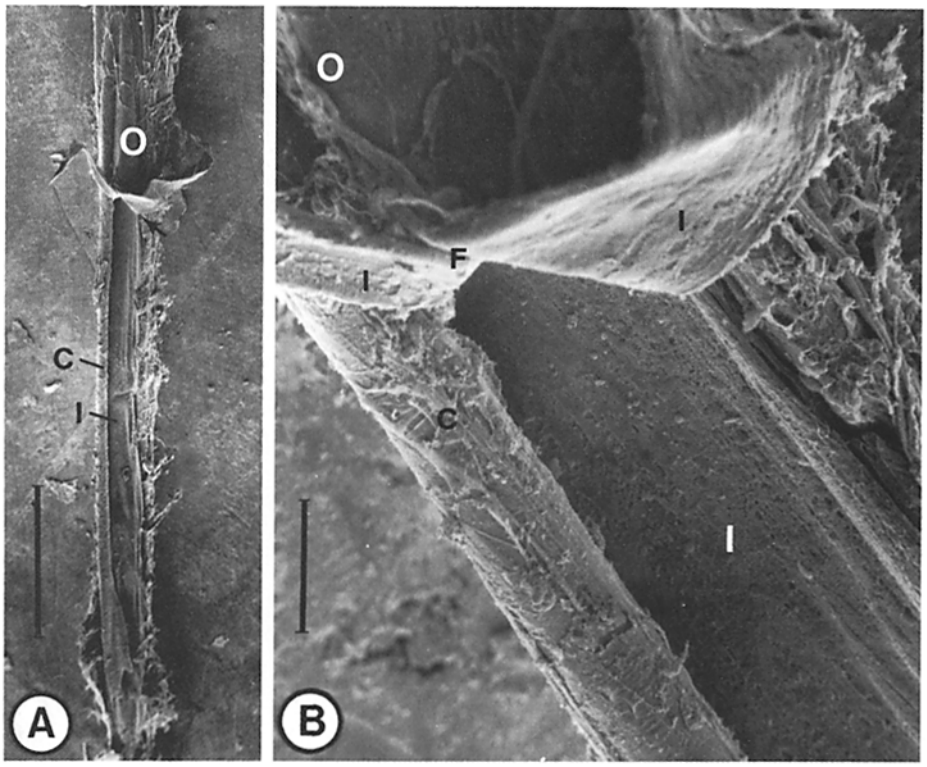

FIGURES 2–8 Scanning electron micrographs of the perfusion zone of intracellularly perfused squid giant nerve fibers. Procedures used for perfusion and microscopy are described in Materials and Methods.

FIGURE 2 Surveys: the inner face (*I*) of ther perfused portion; the outer face (*O*) and the sectioned part (*C*) of the fiber wall. The end of the opened portion of the perfused zone is shown at higher magnification in Fig. 2*B*: flaps (*F*) of the resected upper half of the perfused fiber are folded backwards, exposing the axoplasmic face of the flaps. (*A*) Bar, 1 mm. × 20. (*B*) Bar, 0.1 mm. × 180.

phate solution without pronase, the ectoplasm of fibers briefly perfused with pronase appears as a distinct, three-dimensional network. It therefore appears that pronase is digesting, during the first several minutes of perfusion, primarily interfilamentous proteins.

PRONASE PERFUSION RESULTING IN SUPPRESSION OF EXCITABILITY: Intracellular perfusion with 0.3 mg/ml pronase brought about repetitive firing (see Fig. 9B), interrupted by an intermittent conduction block (not included in the record of Fig. 9B). The empty inner space and the even inner aspect of the preparation is clearly demonstrated in survey micrographs of fibers after such a perfusion (Fig. 5*A*). At higher magnification, the inner aspect of the preparation appears to be covered with blebs distributed evenly over the entire area in the perfused zone (Fig. 5*B*). Further increase of magnification discloses a detailed and highly revealing morphology of the inner aspect of the axolemma and of the adjoining ectoplasm (Fig. 6). Numerous smooth-surfaced profiles can be seen on the inner face of the perfused axon as well as individual and aggregated blebs. A densely interwoven meshwork of ectoplasm filaments still covers a considerable part of the axolemma. However, areas of axolemma with only individual filaments and granules attached or completely free of any attachments do occur. Occasionally, individual ectoplasm filaments extend from the dense meshwork and associate with the smooth profiles (arrow, Fig. 6). The smooth profiles have bulbous, fingerlike, and tubular shapes. Occasionally they appear to be continuous with the smooth area of the supposed axolemma.

In fibers in which the excitability was suppressed completely after pronase perfusion (see Fig. 9F), approximately one-third of the inner face of the axolemma is free of filaments and appears smooth (Fig. 7*A*). Blebs and smooth

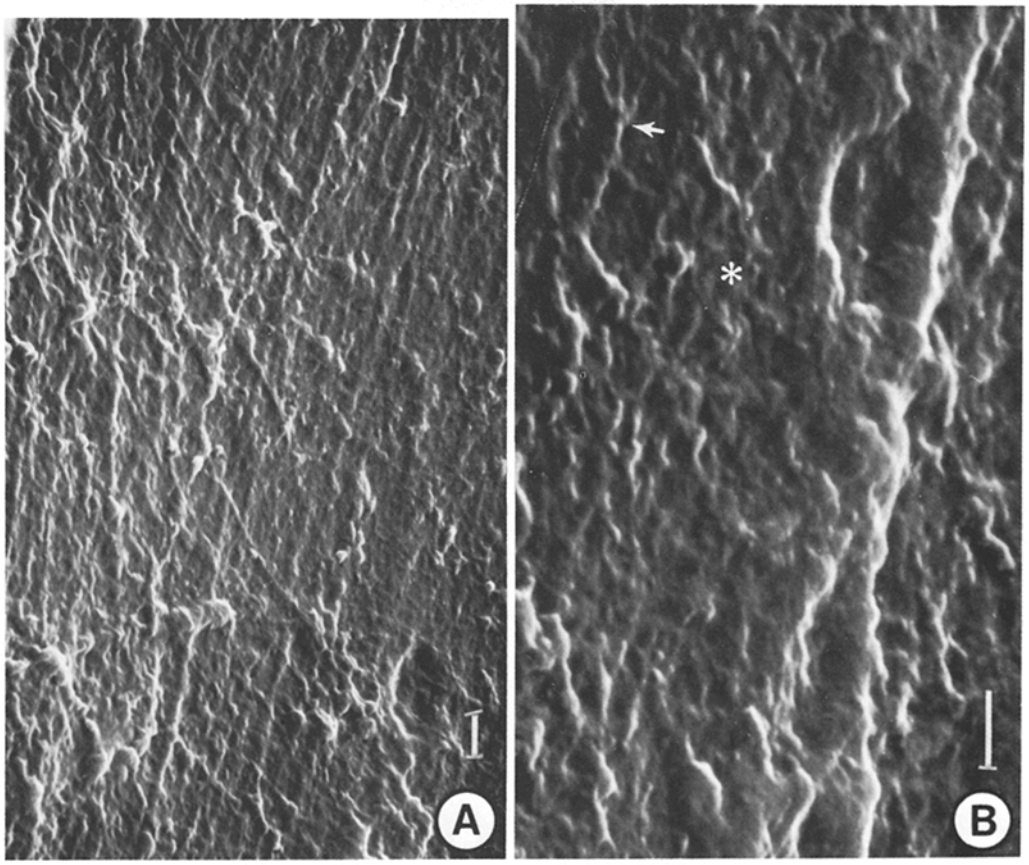

FIGURE 3 Inner face of the ectoplasm in a fiber perfused with KF-phosphate for 50 min. The longitudinal axis of the fiber is parallel to the vertical margin of the figures. (*A*) Predominantly straight threadlike elements, ~0.3 μm in diameter, are associated in a cross-lattice pattern. Bar, 1 μm. × 5,000. (*B*) Matlike assembly of wavy and curved threads (asterisk), ~0.1 μm in diameter, which are interwoven in a network. The predominant orientations of the network elements are the same as of those in the cross-lattice in Fig. 3*A*. Arrow indicates branching point of a 0.3-μm wide thread into three finer components. Bar, 1 μm. × 10,000.

profiles can be seen in such smooth areas only occasionally. The remaining two-thirds of the inner face of the axolemma is still covered with remnants of a finely meshed network (Fig. 7*B*).

PERFUSION WITH Ca^{++}-CONTAINING SEAWATER: Intracellular perfusion with Ca^{++}-containing artificial seawater suppresses excitability within several seconds after the onset of perfusion. After 24 min of perfusion, the inner aspect of the perfusion zone displays rugged, grape clusterlike structure without any discernible filamentous structures (Fig. 8).

ELECTRICAL RECORDING: During the course of digestion of the axoplasm with proteolytic enzymes, electrophysiological properties of the axon are known to change gradually with time (59). The ability of the axon membrane to develop strong inward current is impaired and the duration of the action potential is increased. Eventually, the ability of the axon to carry a nerve impulse is completely eliminated. The excitability of a fiber is completely suppressed after about 36 min of perfusion with 0.1 mg/ml pronase in KF-phosphate. The action potential changes of the fiber during such a perfusion period are illustrated in Fig. 9.

Transmission Electron Microscopy of Thin Sections

All the observations made by scanning electron microscopy can be correlated with the observa-

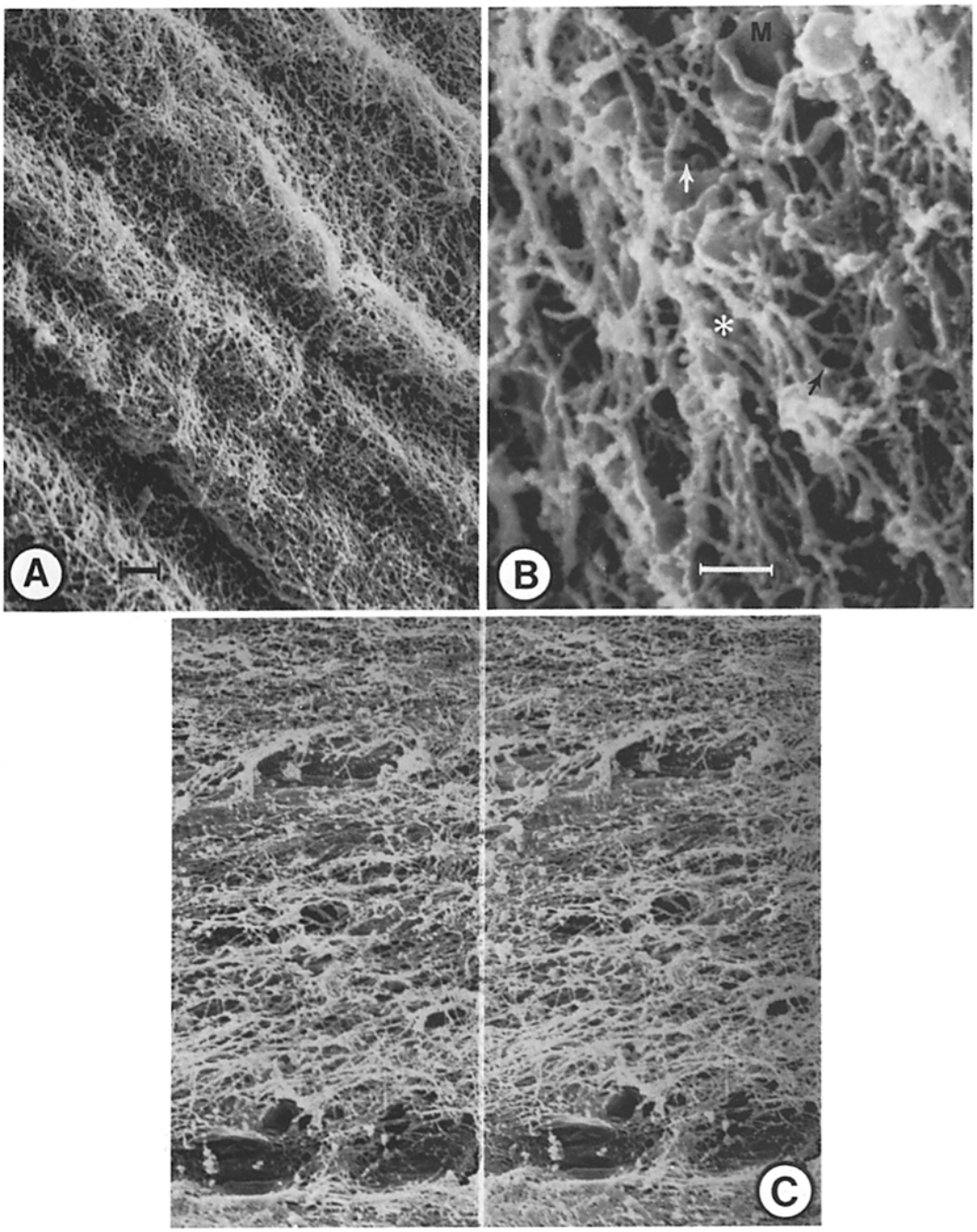

FIGURE 4 A space-network on the inner face of the axolemma. The network is composed of distinct threads interwoven in a continuous three-dimensional structure. The fiber was perfused with pronase (0.1 mg/ml) for 10 min and showed no changes of excitability. (*A*) The inner face of the perfused axon displays alternate ridges and furrows arranged parallel to the long axis of the axon, which is oriented 45° relative to the horizontal line of the figure. Bar, 1 μm. × 5,400. (*B*) Arrows indicate association of threads in a continuous network; beaded threads (asterisks); smooth membrane surface (*M*). Bar, 0.5 μm. × 20,000. (*C*) Stereo-pair micrographs with a 7° difference in tilt; × 6,000. The three-dimensional character of the network can be appreciated by viewing both micrographs with a stereoscope (Hubbard Scientific Co., Northbrook, Illinois) magnifying × 2.2; with a × 2.2 stereoscope × 13,200.

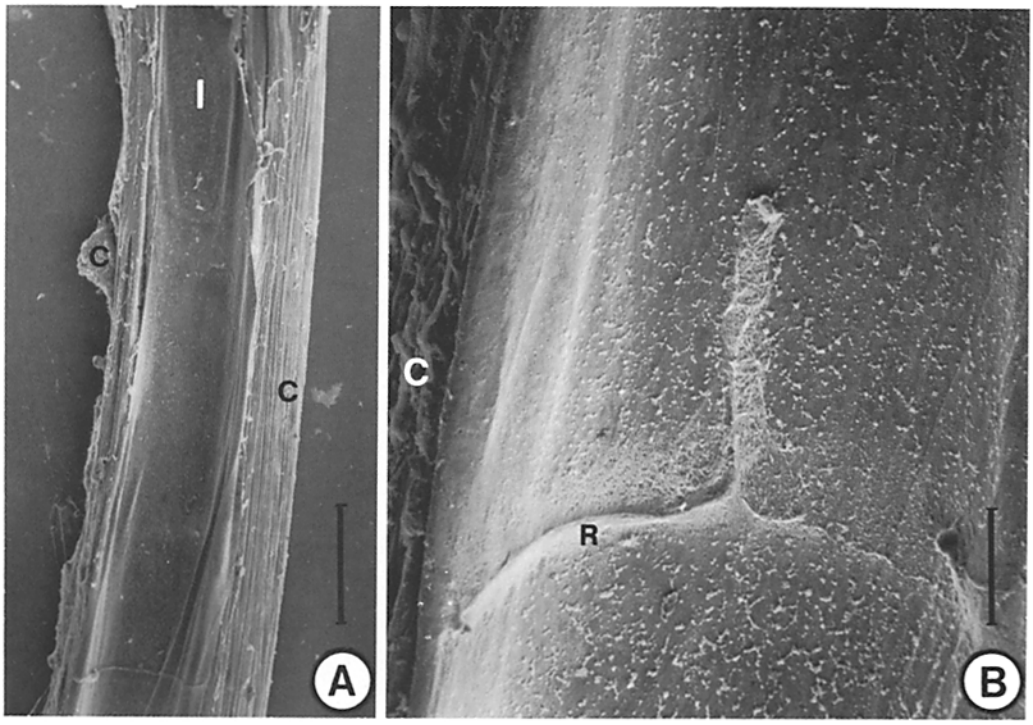

FIGURE 5 Perfusion with pronase (0.18 mg/ml) for 6 min brought repetitive firing. (*A*) The empty perfusion space and the even inner aspect (*I*) of the preparation; layer (*C*) consisting of longitudinally sectioned Schwann sheath, small fibers and connective tissue. Bar, 0.5 mm. × 30. (*B*) Evenly distributed blebs on the inner face of the axolemma. Circular ridgelike elevation (*R*) of ectoplasm remnants extends into a taillike prolongation. Note the striations oriented at ~30° relative to the long axis of the fiber in the right-hand corner of the figure. Bar, 0.1 mm. × 150.

tions of thin sections by transmission electron microscopy. At the resolution used in the present investigation, no significant differences in structure of filamentous and membranous components of the axon could be observed between the fibers fixed either in osmium tetroxide or in paraformaldehyde-glutaraldehyde solutions. This has been observed in intact as well as in perfused fibers. In intact fibers, a network consisting of densely interwoven filaments extends in the ectoplasm. The diameter of the filaments measures ~70 Å and many finer filaments can also be identified. The filaments of this ectoplasmic network appear to be attached to the axolemma (arrows, Fig. 10*A* and *B*); see also Fig. 20 in reference 27. From filaments oriented parallel to the surface of the axon, comblike projections associate with the axolemma (arrowhead, Fig. 10*A*). Short filament fragments of the subaxolemmal network, attached to the axolemma, appear at higher contrast in pronase-perfused fibers (arrow, Fig. 14*C*). Mitochondria occur in close apposition to the axolemma (Fig. 10*B*); see also Fig. 6 in reference 26, where a mitochondrion has been illustrated in a fiber fixed in osmium tetroxide solution. Besides mitochondria, membrane-bounded profiles of agranular endoplasmic reticulum occur in the ectoplasm. Such profiles may be densely packed in large bodies and are observed in fibers fixed in osmium tetroxide as well as in fibers fixed in aldehyde mixture. These structures have been described and illustrated in detail previously: Fig. 7 in reference 26 should be consulted.

Intracellular perfusion with 400 mM KCl blocks the action potential in ~24 min. In the perfused zone of such fibers, the major portion of the inner face of the axolemma is predominantly covered by a well-defined layer of axoplasm. This layer can be up to 0.6 μm thick and is bordered on the side of the structureless perfusion lumen by a rim of condensed axoplasm (Fig. 11*A*). The filamentous network, with filaments attached to the axolemma (arrow, Fig. 11*A*), can be identified in the axoplasm layer, among numerous membranous pro-

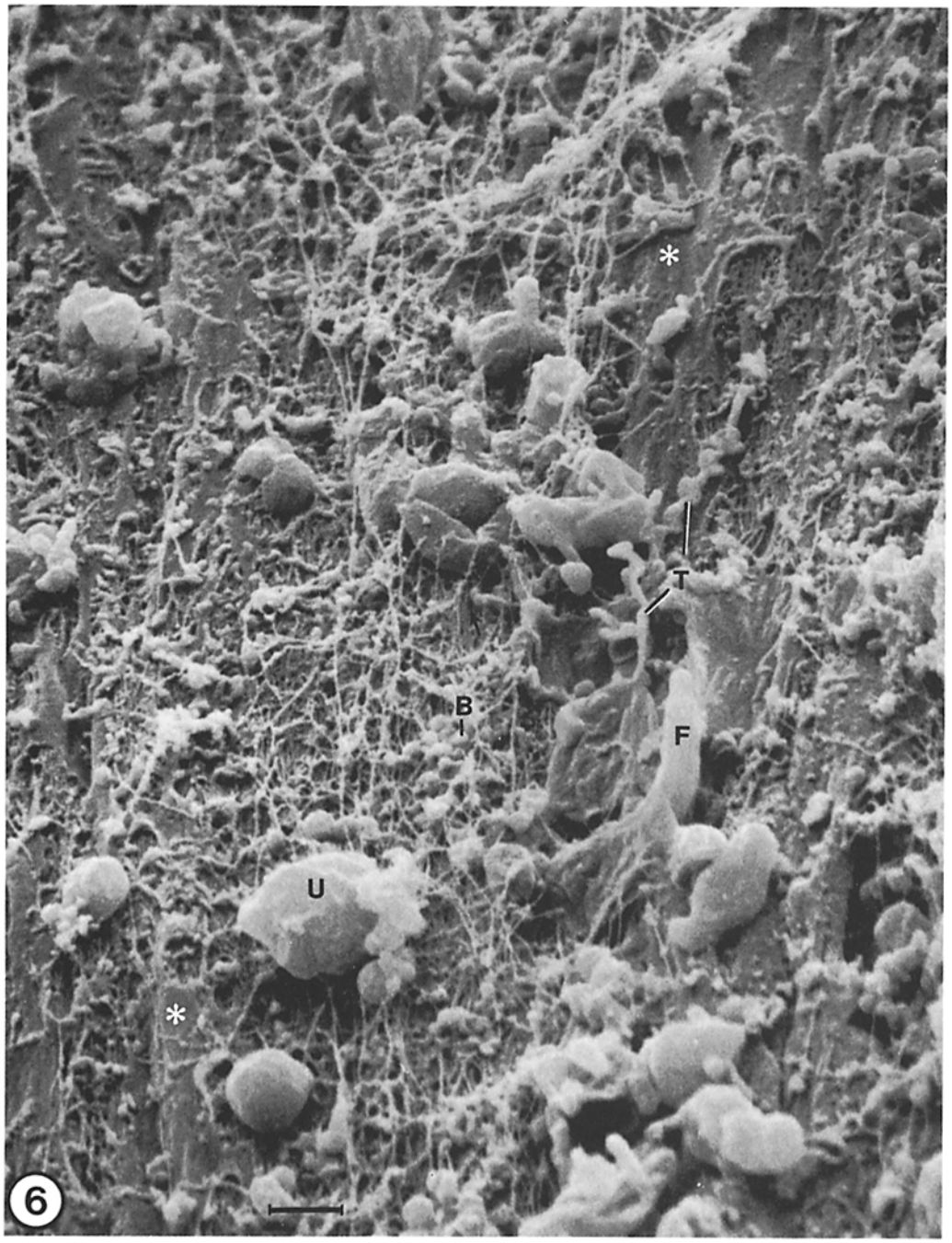

FIGURE 6 Bulbous (*U*), fingerlike (*F*), and tubular (*T*) smooth profiles; aggregates of blebs (*B*) surrounded by the network of ectoplasm filaments. The fingerlike and tubular profiles are continuous with the even portion of the inner face of the preparation, probably the axolemma. Inner face of the supposed axolemma free of attachments (asterisk); filaments extending from the meshwork to smooth profiles (arrow). Perfusion with pronase (0.3 mg/ml) for 6 min resulting in repetitive firing. Bar, 1 μm. × 10,800.

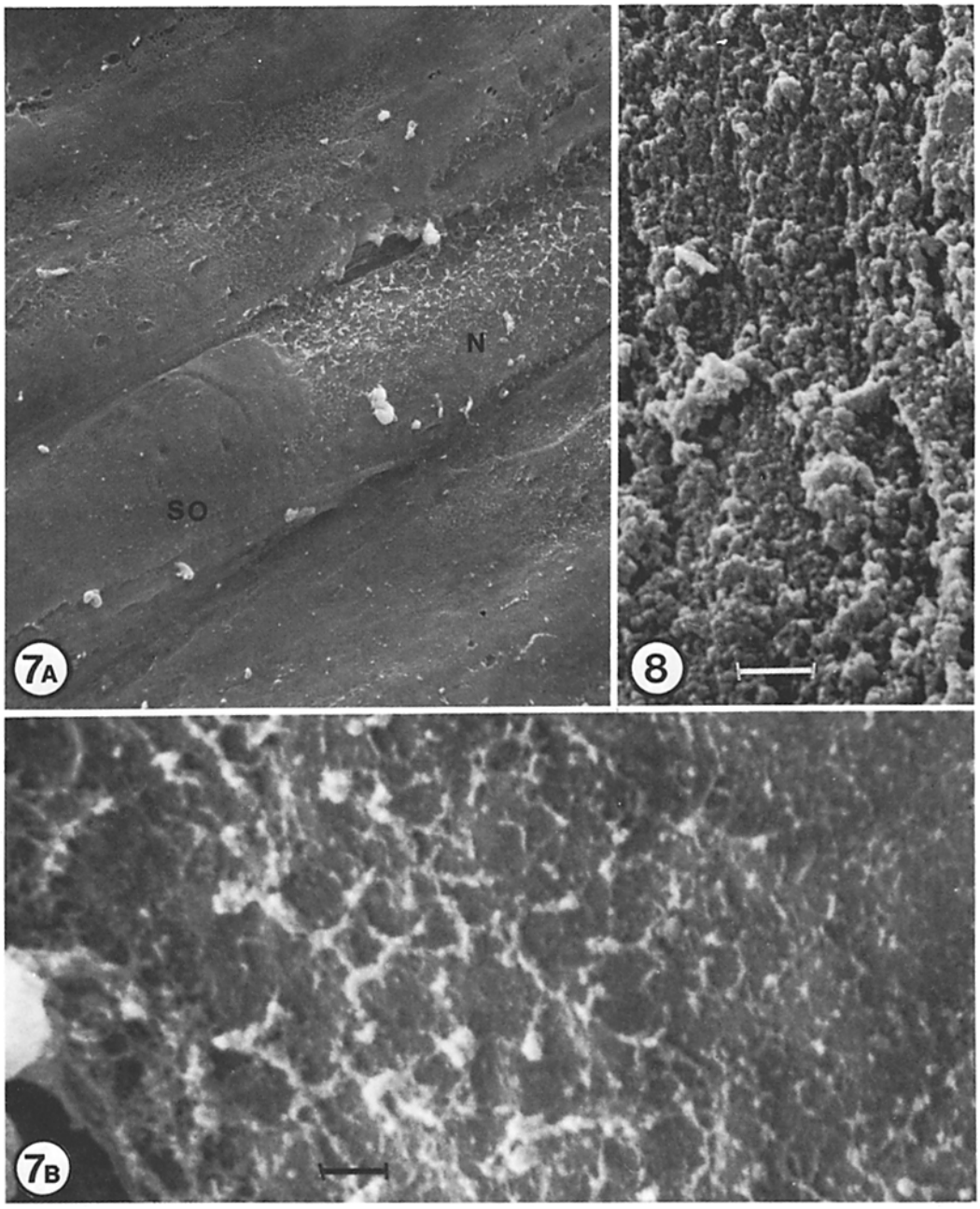

FIGURE 7 Perfusion with pronase (0.1 mg/ml) for 35 min resulting in a complete suppression of excitability. (*A*) Survey of an extensive area of a smooth inner cytoplasmic face of the axolemma without any filaments and granules attached (*SO*). Patches consisting of remnants of subaxolemmal filamentous network (*N*) can be found still associated with the axolemma. A small number of blebs and smooth profiles can be identified. In other areas of the preparation, numerous smooth profiles can be seen. The width of the figure corresponds to 0.4 mm. × 2,200. (*B*) Higher magnification of remnants of the ectoplasmic filamentous network extending on the inner face of the axolemma. The association of the filaments in a network structure is still evident. Bar, 0.5 μm. × 17,500.

FIGURE 8 A rugged, grape clusterlike structure of the inner aspect of a fiber perfused intracellularly for 24 min with Ca^{++} containing artificial seawater. The excitability was blocked ~20 s after the onset of perfusion. Bar, 1 μm. × 10,000.

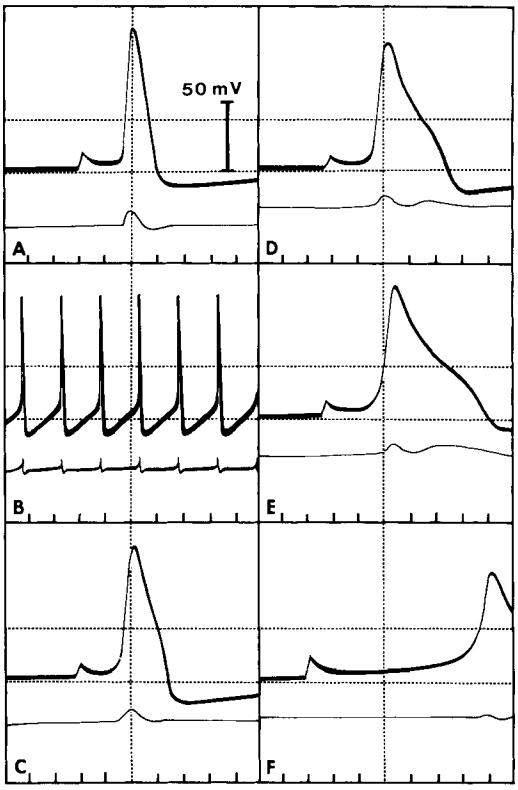

FIGURE 9 Oscilloscope records showing the changes of the action potential during intracellular perfusion with 0.1 mg/ml pronase for 36 min. Start (*A*) and termination (*F*) of perfusion. There is a time interval of 6 min between each figure. The time markers are 1 ms apart.

files and profiles of microtubules. Most interestingly, extensive areas do exist where the inner face of the axolemma is completely free of attached filaments and, thus, is facing directly the structureless perfusion zone or debris of the axoplasm (Fig. 11*B*). In such areas, often the exact nature of the membranous material cannot be identified with certainty anymore. For example, in Fig. 11*C* the identification of the membranous profiles is only tentative. A comparison with Fig. 11*B* is helpful in this respect. Accordingly, Fig. 11*C* may represent membranous material (*M*) of the axoplasm apposing the smooth inner face of the axolemma (*L*). Such areas cannot be seen in intact fibers. Any interruption in the continuity of the axolemma could not be detected in the fiber perfused with KCl.

Subsequent perfusion of fibers for 5 min with Ca^{++}-containing artificial seawater, followed by ~10 min of perfusion with KCl, removes most of the axoplasm from the perfusion zone. The axolemma is often folded and associated with irregular membranous material. No axolemma can be identified over a wide range, and debris of the Schwann cell cytoplasm faces the lumen of perfusion (Fig. 12). Occasionally, a continuous profile of the axolemma can be traced in a narrow range where axoplasmic filaments appear to be still attached to the intact axolemma. Furthermore, filamentous material (arrowhead, Fig. 13) extends across the extracellular space between the axolemma and the adjoining membrane of the Schwann cell (*SL*, Fig. 13). Such material between the axolemma and the plasma membrane of the Schwann cell can be seen in thin sections of all perfused fibers as well as in controls. However, these structures appear most distinctly in fibers perfused with KCl and Ca^{++}-containing seawater.

The perfusion zone of fibers which were treated with pronase until the excitability was completely suppressed has been investigated by thin-section electron microscopy. The intra-axonal perfusion lumen (*PL*, Fig. 14) is surrounded by the axolemma and the adjoining Schwann cell layer. Elevations of the Schwann cell layer into the perfusion lumen are due to the presence of the Schwann cell nuclei and localized thickenings of the Schwann cell cytoplasm, which contains many large vacuoles (Fig. 14). Besides the elevations, numerous bleblike protrusions into the perfusion space characterize the perfusion zone. Such protrusions represent local expansions of the axolemma which have separated over a limited range from the opposing Schwann cell plasma membrane (Fig. 14*A*). Inside the perfusion lumen, smooth membranous material of varying size and shape can be seen (Fig. 14*B*). Indications of possible continuity between the material of the large membranous bodies and the axolemma could be observed on several occasions (Fig. 14*C*). In thin sections of the perfusion zone, portions of the axolemma can be identified which appear smooth and free of axoplasmic filaments. However, in other portions of the perfusion zone, short filament fragments of the subaxolemmal network are still attached to the axoplasmic face of the axolemma (Fig. 14*C*).

In intact fibers, vacuolized Schwann cell cytoplasm, local bleblike protrusions, and membranous structures as illustrated in Fig. 14*B* and *C*, as well as extensive areas of axolemma free of filaments could never be seen. An extensive vacuolization of the Schwann cells can be discerned

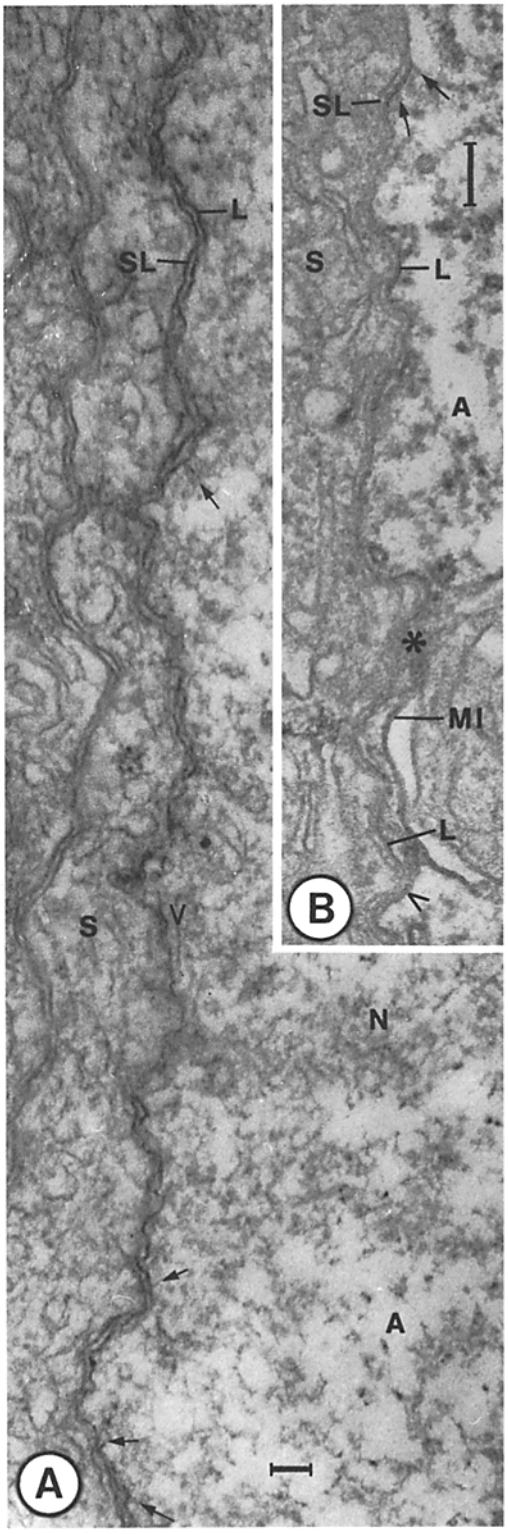

during pronase perfusion even in the dissecting microscope;[2] before the perfusion, such a vacuolization cannot be seen (63).

Localization of Actinlike Filaments by HMM-Binding Experiments

Actinlike filaments can be identified regularly in freshly extruded axoplasm homogenates and in thin sections of glycerinated squid giant nerve fibers following treatment with HMM. Filaments 250–300 Å in width and of variable lengths, displaying characteristic arrowhead pattern, can be observed frequently in axoplasm homogenized in SSS, treated on the grid with HMM, and stained negatively with 1% uranyl acetate (Fig. 15*A* and *B*). Parallel actinlike filaments with arrowheads oriented in opposite directions can be observed in close proximity to each other (Fig. 15*B*, *inset*). Furthermore, in such preparations, actinlike filaments can be observed along which the direction of arrowheads is reversed, indicating a change in polarity of the assembly of G-actin (Fig. 15*C*); see also reference 66. Actinlike filaments displaying arrowhead pattern appear to be continuous with 70-Å filaments of smooth outline (Fig. 15*C*). In control experiments the grid was

[2] I. Tasaki and J. Metuzals, unpublished observations.

FIGURES 10–14 Transmission electron micrographs of transverse thin sections of fibers fixed in 1% glutaraldehyde and 1% paraformaldehyde dissolved in seawater, postfixed in 1% osmium tetroxide, and treated as described in Materials and Methods. The fiber illustrated in Fig. 10*A* was fixed directly in 1% osmium tetroxide at room temperature.

FIGURE 10 Ectoplasmic portion of the axoplasm (*A*) adjoining the axolemma (*L*); cytoplasm (*S*) and plasma membrane (*SL*) of Schwann cells. (A) Filaments of variable diameter but predominantly ~70 Å wide are associated directly with the axolemma at numerous sites (arrows); filament, oriented parallel to the axolemma, is associated with the axolemma by comblike projections (arrowhead); network (*N*) of interwoven filaments in the ectoplasm. Bar, 0.1 μm. × 52,000. (B) Axoplasm filament (arrows) associated with the axolemma. A mitochondrion in juxtaposition to the axolemma; the outer membrane (*MI*) of the mitochondrion. An area (asterisk) where the Schwann cell plasma membrane, the axolemma, and the outer mitochondrial membrane appear indistinct because of changed orientation towards the plane of the section. Another area (arrowhead) where the Schwann cell plasma membrane and the axolemma appear indistinct for the same reasons. Bar, 0.1 μm. × 75,000.

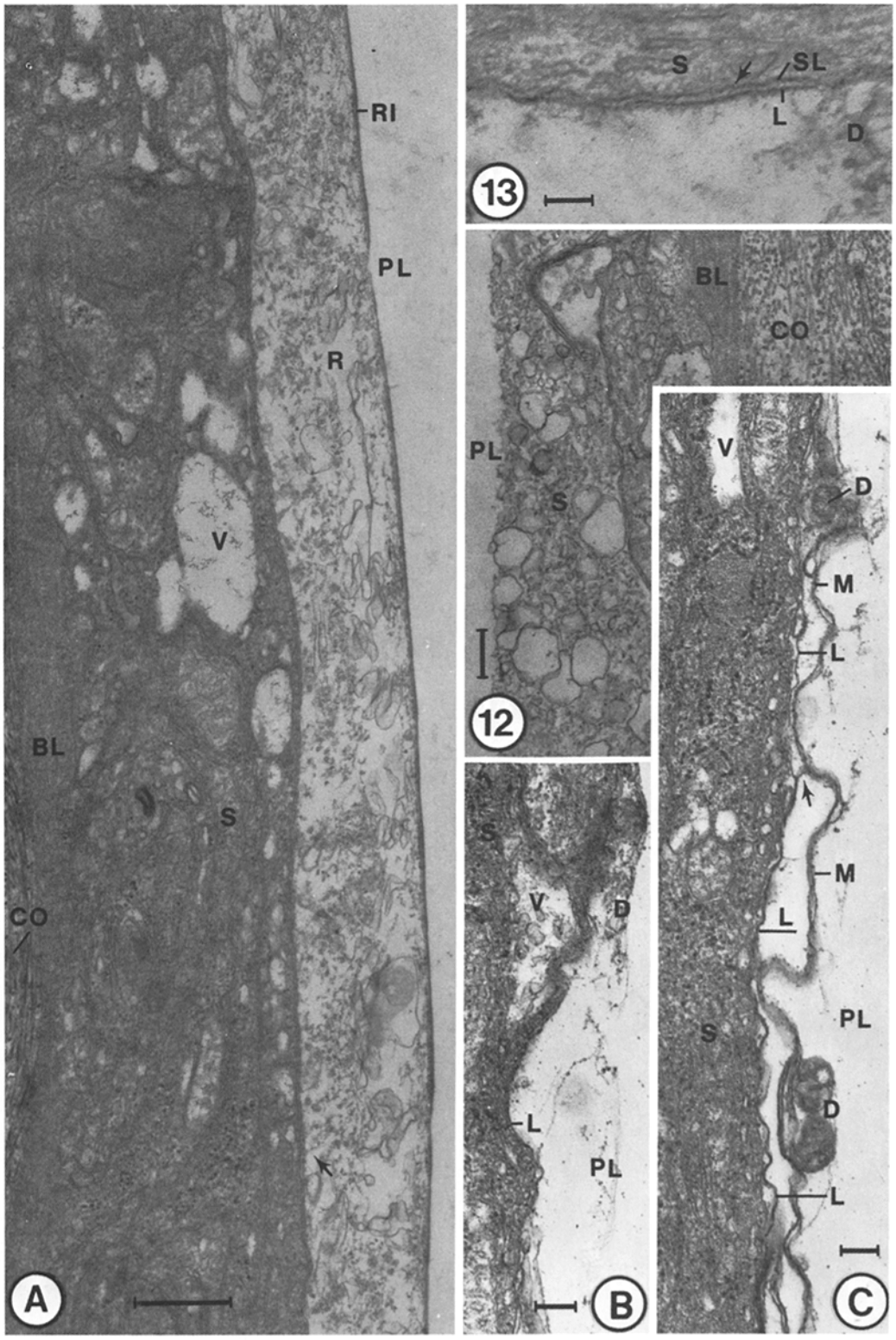
RI
PL
R
V
BL
S
CO
A
S
SL
L
D
13
BL
CO
PL
S
12
V
D
M
L
M
L
PL
S
D
L
V
D
S
L
PL
B
C

rinsed with 10 mM ATP after the treatment with HMM (Fig. 15*D*), or HMM was omitted (Fig. 15*E*). Filaments resembling decorated F-actin were never observed in the controls.

In thin sections of glycerinated, HMM-treated giant nerve fibers, numerous 150–250-Å wide filaments, displaying arrowhead structures characteristic of decorated F-actin filaments, can be identified (Fig. 16). Such actinlike filaments, decorated with HMM, can be identified close to or even in direct contact with the axolemma (Fig. 16*B–E*). The diameter and appearance of these actinlike filaments in thin sections of the axoplasm are identical to those of HMM-decorated muscle F-actin which has been embedded and sectioned under the same experimental conditions; see also reference 28. Control experiments consisted of addition of 10 mM ATP at the beginning of the treatment with HMM. In sections from these controls, filaments resembling decorated F-actin were never observed (Fig. 17).

The decorated actinlike filaments represent only a portion from the total amount of filaments visible in axoplasm homogenates and in glycerinated fibers after treatment with HMM. Numerous filaments, which are not decorated and correspond to the so called neurofilaments, do exist in these preparations.

SDS-Polyacrylamide Gel Electrophoresis

The molecular weight distribution of polypeptides from freshly extruded axoplasm of the squid giant nerve fiber provides a standard of comparison necessary for protein identification and isolation. The gel pattern for total axoplasm is shown in Fig. 18. A comparison of this polyacrylamide gel pattern with that obtained from rabbit skeletal muscle actin indicates that a protein present in axoplasm has a molecular weight identical to that of muscle actin (band *8*, Fig. 18). Bands *7* and *6* (Fig. 18) have a mobility corresponding to a peptide of mol wt ~56,000. Bands *4*, *3*, and *2* in Fig. 18 correspond to mol wt of 70,000, 72,000, and 89,000, respectively.

DISCUSSION

Questions relating to the association of cytoplasmic filaments with the plasma membrane are of primary significance not only in neurobiology but also in the biology and pathology of the cell generally. The squid giant nerve fiber provides unique advantages to investigate these problems from structural, chemical, and functional viewpoints. It is generally accepted that the submembranous network of filamentous proteins provides support to the plasma membrane (55) and a

---

FIGURES 11*A*, *B*, and *C*, and 12 and 13 Segments from the wall of perfused fibers. Layer of the axoplasm (*R*); axolemma (*L*); axoplasmic debris (*D*); structureless perfusion space (*PL*); cytoplasm (*S*) of Schwann cells with vacuoles (*V*); basal lamina (*BL*); layer of collagenous fibers (*CO*).

FIGURE 11 *A*, *B*, and *C* Perfusion with 400 mM KCl for 9 min resulting in suppression of excitability. (*A*) An even rim of condensed axoplasm (*RI*) borders the axoplasm layer against the perfusion space. In the axoplasmic layer, membranous material, filaments, and microtubules can be identified. Individual filaments (arrow) attached to the axolemma can be identified. Bar, 0.5 μm. × 30,000. (*B*) Transition area between disintegrating axoplasmic layer and a region where a smooth inner face of the axolemma, free of attached cytoplasmic filaments, is exposed against the perfusion space. Bar, 0.1 μm. × 62,500. (*C*) Membranous material (*M*) of the axoplasm in apposition to a smooth membrane (*L*). Dense material (arrow) between the membranous material of the axoplasm and the smooth membrane. Bar, 0.1 μm. × 62,500.

FIGURES 12 and 13 Perfusion with 400 mM KCl for 9 min followed by Ca^{++}-containing seawater for 5 min. About 20 s after the onset of seawater perfusion, the action potential was blocked. Bar, 0.1 μm. × 75,000.

FIGURE 12 Schwann cell debris facing the perfusion space because most of the axon and portions of Schwann cells have been removed over a wide range of the perfusion zone.

FIGURE 13 Intact axolemma and Schwann cell plasma membrane can be identified for short distances. Fine filaments (arrow) extend through the extracellular space between the axolemma and the adjoining plasma membrane of the Schwann cell. Short filaments are attached to the cytoplasmic face of the axolemma.

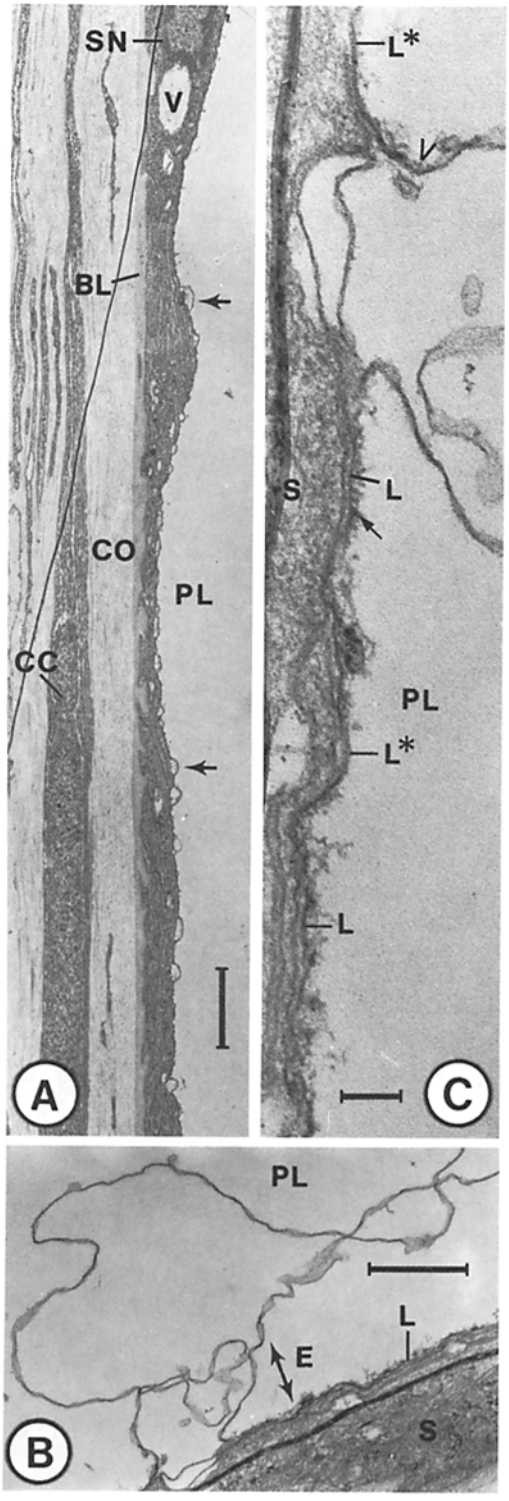

linkage with cytoskeletal components (2, 34, 28). Furthermore, it controls the mobility of protein complexes in the lipid bilayer (46, 37, 52, 51). Thus, a redistribution of intramembrane proteins and other components of the membrane may have a profound consequence on certain membrane-associated functions of the cell and may affect the specific transport of ions as well (5). It has been suggested by Inoué et al. (18) that submembrane structures may be involved in the maintenance of the excitability in the squid axon.

The direct and extensive attachment of subaxolemmal filaments to the axolemma is clearly demonstrated in experiments involving axoplasm removal by suction of a micro-cannula inserted into living fibers. The indentation of the axolemma is always behind and not opposite the orifice of the cannula and corresponds with the site of attachment of a birefringent fanlike structure to the axolemma. Further evidence for the existence of an extensive attachment of ectoplasmic filaments to the axolemma is provided by electron microscopy of thin sections of intact and intracellularly perfused fibers, fixed either in paraformaldehyde-glutaraldehyde or directly in osmium tetroxide solutions. In fibers fixed after perfusion with pronase, areas of axolemma can be identified where fragments of filaments are still attached to it. An *en face* view of a filamentous network is revealed on the inner surface of the axolemma by scanning electron microscopy of fibers after extensive diges-

FIGURE 14 The wall of the perfusion zone of a fiber perfused with pronase (0.1 mg/ml) for 36 min, resulting in suppression of excitability, see Fig. 9. (*A*) Numerous blebs (arrows) of the axolemma protrude into the perfusion space (*PL*) of the axon; nucleus of the Schwann cell (*SN*); vacuole (*V*) in the Schwann cell cytoplasm; basal lamina (*BL*); collagenous fiber layer (*CO*); connective tissue cell (*CC*). Bar, 1 μm. × 10,000. (*B*) Smooth membranous profile protruding into the perfusion space (*PL*). The membrane of the profile forms a necklike (*E*) connection with the main part of the axolemma (*L*). Bar, 0.5 μm. × 25,000. (*C*) Higher magnification of the necklike connection in Fig. 14*B*, illustrating a possible continuity (arrowhead) between the membrane of the profile and the axolemma. The membrane of the profile is free of attached filaments; portions of the axolemma free of filaments (*L**); portions of the axolemma (*L*) with attached short cytoplasmic filaments; short filament fragments (arrow) of the subaxolemmal network attached to the axolemma; Schwann cell cytoplasm (*S*) and perfusion space (*PL*). Bar, 0.1 μm. × 75,000.

tion by internal application of pronase; see also references 8, 4, and 61.

Intracellular perfusion with a KF-phosphate solution does not bring about any changes in the cross-lattice structure of the ectoplasm adjoining the axolemma; no excitability changes can be detected in such fibers. This conclusion is supported by comparing the results of observations made by scanning electron microscopy of KF-perfused fibers (described under section entitled Perfusion with KF-Phosphate), with the finding obtained previously by differential interference microscopy (27). The appearance, dimensions, and angular spread of the threadlike elements are comparable in both types of preparations, in spite of the fact that the specimens for scanning electron microscopy have been fixed, dehydrated, and coated. This comparison demonstrates the reliability of our procedures for scanning electron microscopy and excludes the possibility that the observed configurations may be artifacts.

A direct visualization of the three-dimensional assembly of the filamentous network in the ectoplasm has been achieved by scanning electron microscopy of fibers perfused intracellularly with pronase. The stereo-pair micrographs in particular provide unequivocal evidence for a three-dimensional assembly. This type of configuration of the ectoplasmic network was also deduced from observations made with differential interference microscopy and thin-section electron microscopy (27, 67, 28). Obviously, a three-dimensional visualization of this type of structure was not possible with the latter techniques. Studies on the identification, localization, and reassembly of the protein components of the axoplasmic network are in progress (48).

Buckley (5) investigated critical-point dried cultured whole rat embryo cells by transmission electron microscopy, using stereoscopic techniques. In such preparations, interconnected filaments form a widespread three-dimensional fine-mesh network. The network is attached to the plasma membrane and surrounds all organelles. More than 50 years ago, Koltzoff (20) postulated the existence of a cytoskeleton which could determine cell form and changes in form; see also reference 33.

Interfilamentous protein material is removed during the early phase of pronase perfusion, resulting in a distinct delineation and detailed resolution of the threadlike elements in scanning electron micrographs. The beaded appearance and association into wider threads are clearly visible in such preparations, confirming the observations made with negatively stained samples of freshly extruded axoplasm; see also reference 26. In fibers from which the endoplasm has been removed by suction only, the ectoplasm displays bubblelike elevations and smooth surfaces with barely discernible threadlike elements.

Repetitive firing of action potentials during pronase perfusion appears to coincide with the appearance of smooth-surfaced blebs, many vesicles, and large profiles on the inner face of the axolemma. Significantly, the vesicles and the large profiles, as well as many of the blebs, are mostly free of filaments. However, a dense meshwork of subaxolemmal filaments can still be seen over wide areas of the inner face of the axolemma. The possibility can be excluded that the smooth-surfaced blebs, vesicles, and the large profiles observed in our material are fixation artifacts; see reference 47. Such structures cannot be observed in thin sections of intact fibers which have been used as controls. The axolemma in these control fibers may display a slightly wavy course; yet, attached filaments can be identified all over the cytoplasmic face of the axolemma in fibers fixed either in aldehyde mixtures (Fig. 10*B*) or directly in osmium tetroxide (Fig. 10*A*). In thin sections of fibers perfused with KCl, the axolemma appears straight in areas covered by a layer of axoplasm containing filaments attached to the axolemma (Fig. 11*A*). In areas where the filamentous axoplasm components have been removed, a blebbed appearance of the axoplasm is evident (Fig. 11*B* and *C*). Furthermore, indications of close morphological contacts, or even possible continuities between the axolemma and the membranous bodies protruding into the perfusion space (Fig. 14*C*), can be seen. Besides the intact fibers, other controls of the perfusion experiments are the areas in the perfusion zone of perfused fibers, where filaments are still attached to the axolemma. Thus, the possibility can be excluded with certainty that the morphology of the axolemma in filament-free areas of the perfusion zone might be caused through mechanical damage during the initial suction of the endoplasm or during the fixation, dehydration, and final preparation of the perfused fiber for electron microscopy. From these observations, it can be hypothesized that removal of the subaxolemmal

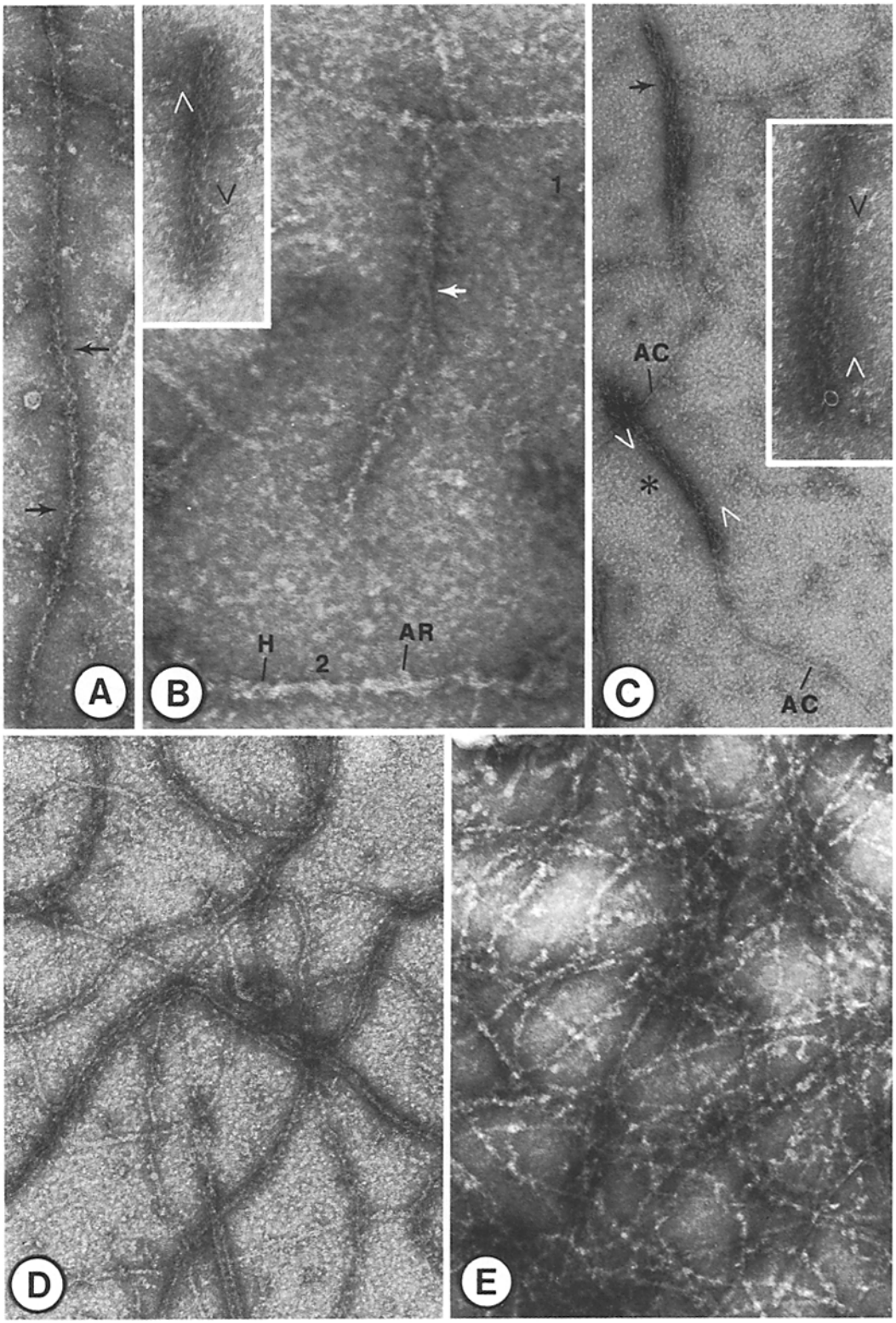
A
B
1
H
2
AR
C
AC
AC
D
E

filaments from restricted areas on the inner face of the axolemma may cause structural destabilization of the axolemmal components with consequent blebbing and fusion with membranous material of the perfusion space. Selective elution of the major component of the submembrane microfilament network, spectrin, is accompanied by the breakdown of the erythrocyte ghosts by endocytic vesiculation (24, 25, 56, 43, 35, 10).

The membranous material in the perfusion space probably originates from disrupted mitochondria and smooth endoplasmic reticulum. It is a well-known fact that, in intact axons of the giant nerve fibers of the squid, mitochondria and profiles of the smooth endoplasmic reticulum appear often in close proximity to the axolemma. Mitochondria apposing the axolemma or even "connected with the Schwann cell cytoplasm" were first observed in intact fibers by Geren and Schmitt (15). In fibers from which the axoplasm has been extruded mechanically and subsequently replaced by a K-salt solution, numerous vesicles have been noted in proximity of the axolemma (3). Baker et al. (3) suggested that these vesicles may originate from damaged mitochondria and other membrane-bounded structures of the axon. In fibers perfused with pronase, endocytic protrusions of the axolemma have been interpreted by Takenaka et al. (58) as fixation artifacts. Processes of Schwann cell layer projecting into the axon have been seen by several authors (15, 3, 58). However, according to our results, the formation by the axolemma of endocytic protrusions into the perfusion space during perfusion with pronase has to be considered, too.

The blebs, microvilli, and other small projections, observed by scanning electron microscopy on the surface of dividing Chinese hamster ovary cells (41), resemble the structures observed on the inner face of the axolemma during pronase perfusion. Multiple lateral blebs have been observed by Costero and Pomerat (9) along the dendrites of nerve cells grown in tissue culture. They appear repetitively and in large numbers in very long segments of the neuronal processes, disappearing as rapidly as they are formed. The authors have referred to this phenomenon as zeiosis. It is reasonable to speculate that the formation of exocytic blebs and excrescences is the consequence of localized destabilization of the plasma membrane, caused by disassembly of submembranous filaments.

In the neuromuscular junction, specialization in the cortex of the juxtaneuronal portions of the junctional folds has been revealed as a branching ladderlike filamentous network (11). These filaments have been considered to be involved in restricting the mobility of receptor proteins to the perineuronal aspects of the postsynaptic membrane. It is conceivable that the distribution and relative immobility of certain protein and lipid components in the axolemma of the squid giant nerve fiber are critical factors in the maintenance of excitability. The maintenance of a specific topography of these membrane components in the axolemma may occur through their attachment to the subaxolemmal network. In perfused fibers which have lost the capacity to generate action potential, the subaxolemmal network has been removed in one-third of the perfusion zone.

A transmission electron microscope study of thin sections of squid axons perfused with pronase

FIGURE 15 Actinlike filaments displaying arrowhead pattern (arrows) after labeling with HMM, and controls. Axoplasm from three fibers extruded into 0.5 ml of SSS, homogenized, and the suspension placed on a grid for 2 min, treated with HMM (400 μg/ml in SSS) for 5 min on the grid, rinsed with 0.1 M KCl, and stained negatively with 1% uranyl acetate, pH 4.4, for 1 min. Control specimens (*D*) were prepared in the same way, except that the rinsing solution contained 10 mM ATP. Another series of control specimens (*E*) were prepared in the same way, except that treatment with HMM and ATP was omitted. (*A, C, D,* and *E*) × 75,000. (*B*) Fundamental differences between an actinlike filament (arrow) and filaments not labeled with HMM; ~70-Å wide filament (*1*) and a filament measuring 100-250 Å in diameter (*2*). Helical substructure (*H*) and lateral projections (*AR*) in filament *2*. × 150,000. *Inset*: Two parallel actinlike filaments with arrowheads oriented in opposite directions (arrowhead, inverted arrowhead). × 75,000. (*C*) Actinlike filaments, displaying arrowhead pattern, continuous with ~70-Å wide filaments (*AC*). Reversal (asterisk) of the direction of arrowheads (arrowhead, inverted arrowhead) in the same filament; reversal also shown in the *inset*. × 75,000. (*D*) Control. After rinsing with 10 mM ATP in SSS, filaments resembling actinlike filaments with arrowhead pattern cannot be seen. Bar, 0.1 μm. × 75,000. (*E*) Control. In negatively stained preparations of axoplasm extruded in SSS and not treated with HMM, filaments displaying arrowhead pattern cannot be seen. Bar, 0.1 μm. × 75,000.

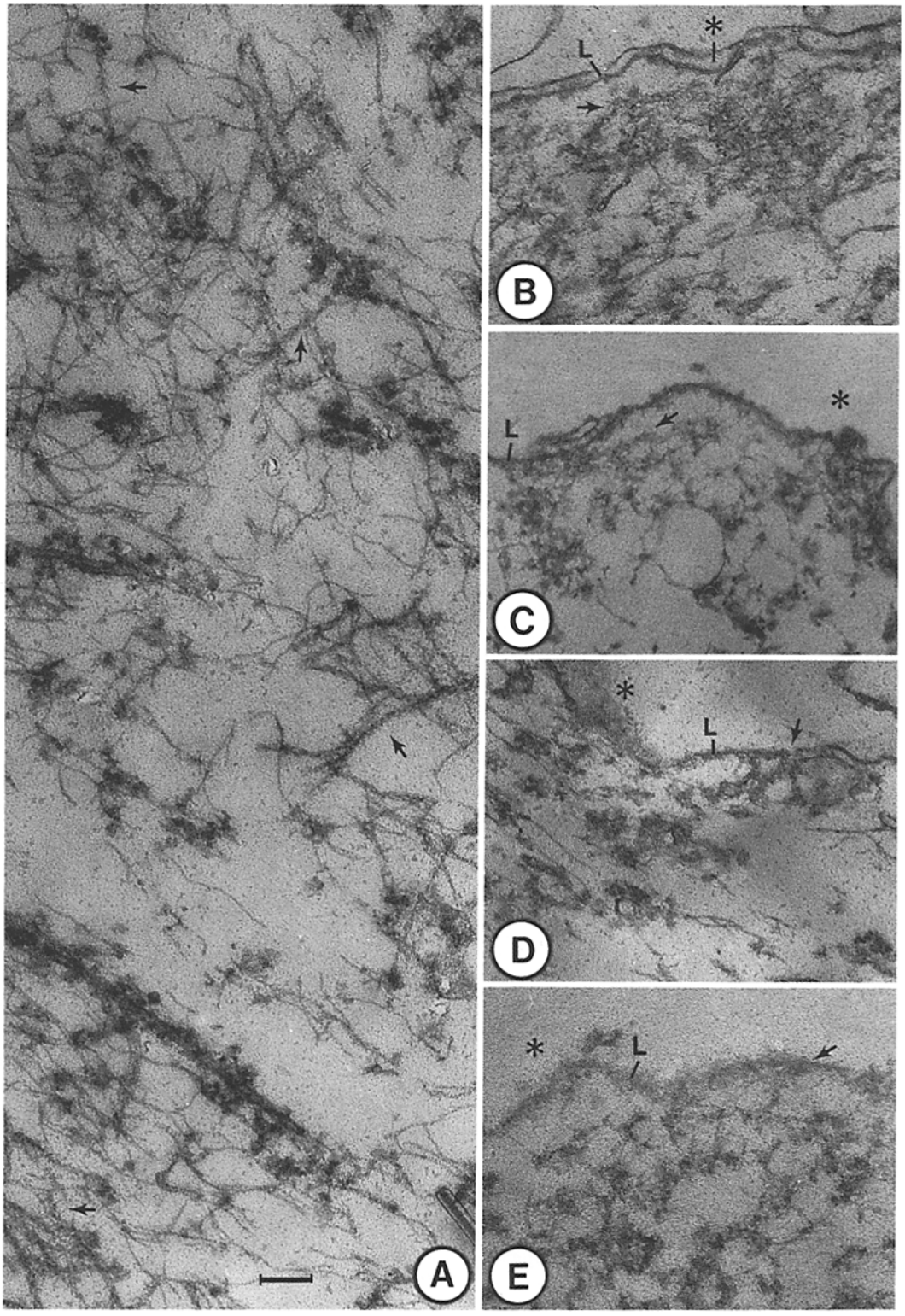

FIGURE 16 Actinlike filaments displaying arrowhead pattern (arrows) after labeling with HMM. Thin sections of the axoplasm from a glycerinated squid giant fiber, fixed and embedded as described in Materials and Methods. Bar, 0.1 μm. × 75,000. (*B–E*) Close proximity and direct contact between the actinlike filaments, labeled with HMM (arrows), and the axolemma (*L*). Extracellular space (asterisk).

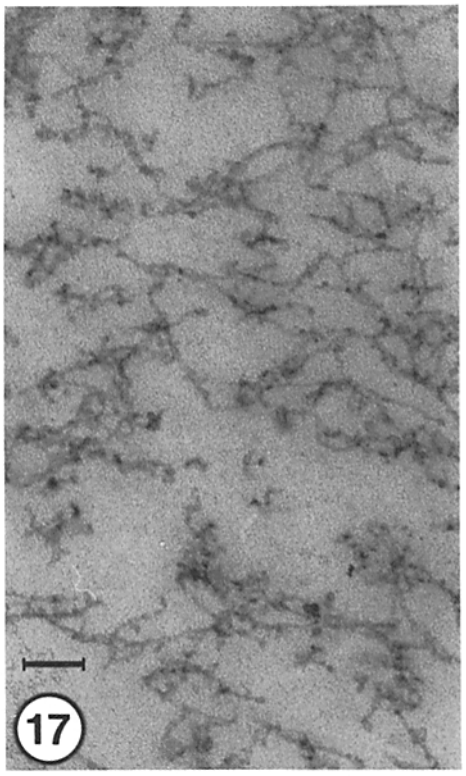

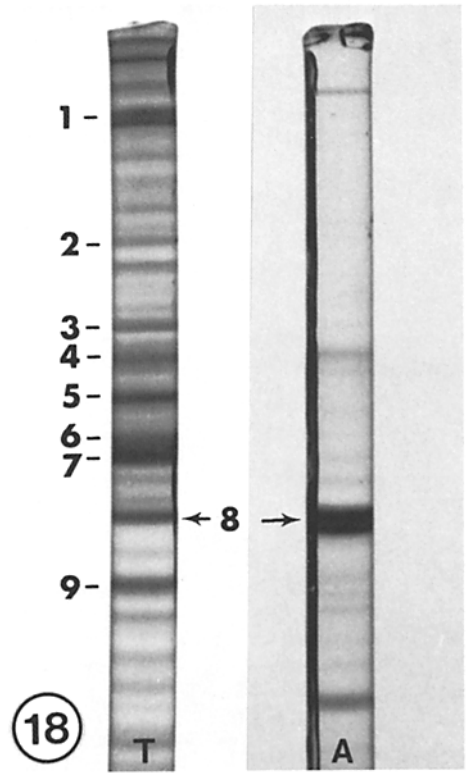

was made by Takenaka et al. (58). In disagreement with our observations, these authors claim that normal action potentials can be obtained after complete removal of the axoplasm. This discrepancy cannot be settled by the results of transmission electron microscopy alone, due to the limited sampling obtainable by thin sectioning of a 15-mm long and 0.5-mm wide perfused zone of the axon. The scanning electron microscopy technique developed in the present investigation provides an overall view of the perfused zone combined with detailed information on the morphology of the inner surface. The technique may be of value in future investigations of the excitable layer in the squid giant nerve fiber (see, for example, reference 1).

The dramatic effect of intracellular perfusion with Ca^{++}-containing seawater is interesting in view of the fact that the same solution has no harmful effect on the outer surface of the fiber. Several factors may be causally involved (see references 16–18 and 36). However, further control experiments are needed to correlate our observations with the data available in the literature. Nevertheless, fibers perfused intracellularly with Ca^{++}-containing seawater provide examples of scanning electron micrographs of disrupted samples. In other experiments, the disruption could be caused by poor fixation and preservation technique.

We have established the presence of actinlike protein in the axoplasm of squid giant nerve fiber using the techniques of HMM-labeling and SDS gel electrophoresis (40, 38). Freshly extruded axoplasm treated with HMM displays actinlike

FIGURE 17 Control. Thin sections of the axoplasm of squid giant nerve fiber treated as the fiber in Fig. 16, except that the fiber in Fig. 17 was incubated with HMM in the presence of 10 mM ATP in SSS. Filaments displaying arrowhead pattern, as illustrated in Fig. 16*A–E*, cannot be seen. Bar, 0.1 μm. × 75,000.

FIGURE 18 Comparison of polypeptide profile of whole axoplasm (*T*) with that of actin isolated from rabbit skeletal muscle (*A*). Both samples were run in 10% polyacrylamide gels under the same conditions. A polypeptide is present in the axoplasm which has a mobility identical to that of the muscle actin (band *8*). The molecular weights of the numbered bands on the *T* gel are: *1* (122,000), *2* (89,000), *3* (72,000), *4* (70,000), *5* (62,000), *6* (56,000), *7* (55,000), *8* (46,000), and *9* (40,000). The molecular weight of the major band in gel *A* (band *8*) is 46,000 and corresponds to that of muscle actin.

filaments decorated in the characteristic arrowhead pattern. In axoplasm homogenates, actinlike filaments can be found arranged side by side. In such a two-filament complex, the orientation of the arrowheads in one filament is opposite to their orientation in the other. Such an arrangement supports the sliding filament model (53), but an artificial origin of such structures in homogenized samples is always possible. Filaments decorated with HMM can be identified in which the orientation of the arrowheads is reversed. It cannot be decided presently whether the images of polarity reversal are produced by two superimposed filaments or else represent intrinsic properties of the filament.

Numerous filaments decorated with HMM can also be identified in thin sections of fixed fibers which have been glycerinated and treated with HMM according to the method of Ishikawa et al. (19). Evidently, the arrowhead pattern of actinlike filaments is never displayed in such preparations so conspicuously and regularly as in negatively stained samples. Stretches of fuzzy attachments can be seen in addition to definite arrowhead structures, a fact noted by all investigators familiar with these techniques (28, 22). In such preparations, actinlike filaments decorated with HMM can be identified either in close proximity to or in a direct contact with the axolemma. However, the number of filaments associated with the axolemma in glycerinated fibers is conspicuously lower than in fibers fixed and treated according to standard procedures. Obviously, glycerol treatment removes material from the axoplasm and distorts the axolemma. In glycerinated control fibers which have not been treated with HMM or in which HMM treatment has been carried out in the presence of ATP, decorated filaments could never be identified.

In both types of preparations treated with HMM—the negatively stained homogenates of axoplasm and the glycerinated fibers—the bulk of filaments are not decorated by HMM and represent the so-called neurofilaments.

By use of the technique of HMM-decoration, actinlike protein has been localized in the axoplasm of glycerinated neuroblastoma cells (6, 7), in central neurons of rat brain (22), and in synapses of rabbit brain (28); see also reference 13. The relatively indistinct appearance of the decorated filaments in glycerinated squid giant fibers may be partly due to the thick connective tissue layer surrounding the axon. However, the appearance of the actinlike filaments as illustrated in the present report is comparable to the appearance of decorated actinlike filaments in other papers (see, for example, references 6, 44, and 28).

The HMM-decoration experiments are supported by the results of SDS-polyacrylamide gel electrophoresis of freshly extruded axoplasm. In gels of the whole axoplasm, a major band can be identified which has a mobility similar to that of rabbit muscle actin. A similar band is also present in gels of intracellular axonal perfusate obtainable from excitable fibers.[3] The results of SDS gel electrophoresis of intracellular perfusates preclude the possibility of an extra-axonal source of actinlike protein. A band with an apparent mol wt of 46,000 has also been identified in extruded axoplasm of squid giant fibers by other workers (14).

Submembrane filaments attached to the plasma membrane have been observed in many types of cells, and in many instances these filaments have been identified as actinlike protein (39, 53, 44, 65, 32, 22, 8, 62). Actin filaments bind to purified lipids under physiological conditions (49). The detailed localization of the actin filaments in the ectoplasm network, their precise relationships with other filamentous components of the axoplasm and with the axolemma, as well as the role which actin may play in excitability and other functions of the axon, remain to be determined in future investigations of the squid giant nerve fiber.

The authors are grateful for constructive criticism on the manuscript made by Drs. W. E. Mushynski, Th. D. Pollard, and R. E. Stephens. The expert technical assistance of Mr. P. Chow-Chong is gratefully acknowledged.

This work was supported by grant MA-1247 from the Medical Research Council of Canada.

Received for publication 13 May 1977, and in revised form 14 February 1978.

REFERENCES

1. Armstrong, C. M., F. Bezanilla, and E. Rojas. 1973. Destruction of sodium conductance inactivation in squid axon perfused with Pronase. *J. Gen. Physiol.* **62**:375–391.
2. Ash, J. F., and S. J. Singer. 1976. Concanavalin-A-induced transmembrane linkage of concanavalin A surface receptors to intracellular myosin-containing filaments. *Proc. Natl. Acad. Sci. U. S. A.* **73**:4575–4579.

[3] J. Baumgold, personal communication.

3. BAKER, P. F., A. L. HODGKIN, and T. I. SHAW. 1962. Replacement of the axoplasm of giant nerve fibers with artificial solutions. *J. Physiol. (Lond.)*. **164**:330–354.
4. BOYLES, J., and D. F. BAINTON. 1975. SEM of filament bundles on the cytoplasmic surface of PMN plasma membrane during phagocytosis. *J. Cell Biol.* **67** (2, Pt. 2):40*a*. (Abstr.).
5. BUCKLEY, I. K. 1975. Three dimensional fine structure of cultured cells: possible implications for subcellular motility. *Tissue Cell.* **7**:51–72.
6. BURTON, P. R., and W. L. KIRKLAND. 1972. Actin detected in mouse neuroblastoma cells by binding of heavy meromyosin. *Nat. New Biol.* **239**:244–246.
7. CHANG, CH.-M., and R. D. GOLDMAN. 1973. The localization of actin-like fibers in cultured neuroblastoma cells as revealed by heavy meromyosin binding. *J. Cell Biol.* **57**:867–874.
8. CLARKE, M., G. SCHATTEN, D. MAZIA, and J. A. SPUDICH. 1975. Visualization of actin fibers associated with the cell membrane in amoebae of *Dictyostelium discoideum*. *Proc. Natl. Acad. Sci. U. S. A.* **72**:1758–1762.
9. COSTERO, I., and C. M. POMERAT. 1951. Cultivation of neurons from the adult human cerebral and cerebellar cortex. *Am. J. Anat.* **89**:405–467.
10. ELGSAETER, A., and D. BRANTON. 1974. Intramembrane particle aggregation in erythrocyte ghosts. I. The effects of protein removal. *J. Cell Biol.* **63**:1018–1030.
11. ELLISMAN, M. H., J. E. RASH, L. A. STAEHELIN, and K. R. PORTER. 1976. Studies of excitable membranes. II. A comparison of specialization at neuromuscular junctions and nonjunctional sarcolemmas of mammalian fast and slow twitch muscle fibers. *J. Cell Biol.* **68**:752–774.
12. FAIRBANKS, G., T. L. STECK, and D. F. H. WALLACH. 1971. Electrophoretic analysis of the major polypeptides of the human erythrocyte membrane. *Biochemistry*. **10**:2606–2617.
13. FINE, R. E., and D. BRAY. 1971. Actin in growing nerve cells. *Nat. New Biol.* **234**:115–118.
14. GAINER, H., and V. S. GAINER. 1976. Proteins in the squid giant axon. *In* Electrobiology of Nerve, Synapse, and Muscle. J. P. Reuben, D. P. Purpura, M. V. L. Bennett, and E. R. Kandel, editors. Raven Press, New York. 155–168.
15. GEREN, B. B., and F. O. SCHMITT. 1954. The structure of the Schwann cell and its relation to the axon in certain invertebrate nerve fibers. *Proc. Natl. Acad. Sci. U. S. A.* **40**:863–870.
16. GILBERT, D. S., B. J. NEWBY, and B. H. ANDERTON. 1975. Neurofilament disguise, destruction and discipline. *Nature (Lond.)*. **256**:586–589.
17. HODGKIN, A. L., and B. KATZ. 1949. The effect of calcium on the axoplasm of giant nerve fibers. *J. Exp. Biol.* **26**:292–294.
18. INOUÉ, I., H. C. PANT, I. TASAKI, and H. GAINER. 1976. Release of proteins from the inner surface of squid axon membrane labeled with tritiated *N*-ethylmaleimide. *J. Gen. Physiol.* **68**:385–395.
19. ISHIKAWA, H., R. BISCHOFF, and H. HOLTZER. 1969. Formation of arrowhead complexes with heavy meromyosin in a variety of cell types. *J. Cell Biol.* **43**:312–328.
20. KOLTZOFF, N. K. 1928. Physikalisch-chemische Grundlage der Morphologie. *Biol. Zentralbl.* **48**:345–369.
21. LAEMMLI, U. K. 1970. Cleavage of structural proteins during the assembly of the Head of Bacteriophage T4. *Nature (Lond.)*. **227**:680–685.
22. LEBEUX, Y. J., and J. WILLEMOT. 1975. An Ultrastructural Study of the Microfilaments in Rat Brain by Means of Heavy Meromyosin labeling. I. The Perikaryon, the Dendrites and the Axon. *Cell Tissue Res.* **160**:1–36.
23. LOWEY, S., and C. COHEN. 1962. Studies on the structure of myosin. *J. Mol. Biol.* **4**:293–308.
24. MARCHESI, V. T., and E. STEERS, JR. 1968. Selective solubilization of a protein component of the red cell membrane. *Science (Wash. D. C.)*. **159**:203–204.
25. MARCHESI, V. T., E. STEERS, T. W. TILLACK, and S. L. MARCHESI. 1969. Some properties of spectrin. A fibrous protein isolated from red cell membranes. *In* Red Cell Membrane. Structure & Function. G. A. Jamieson and T. J. Greenwalt, editors. J. B. Lippincott Co., Philadelphia. 117–130.
26. METUZALS, J. 1969. Configuration of a filamentous network in the axoplasm of the squid (*Loligo pealii* L.) giant nerve fiber. *J. Cell Biol.* **43**:480–505.
27. METUZALS, J. and C. S. IZZARD. 1969. Spatial patterns of threadlike elements in the axoplasm of the giant nerve fiber of the squid (*Loligo pealii* L.) as disclosed by differential interference microscopy and by electron microscopy. *J. Cell Biol.* **43**:456–479.
28. METUZALS, J., and W. E. MUSHYNSKI. 1974. Electron microscope and experimental investigations of the neurofilamentous network in Deiters' neurons. Relationship with the cell surface and nuclear pores. *J. Cell Biol.* **61**:701–722.
29. METUZALS, J., and W. E. MUSHYNSKI. 1974. Filamentous network of the axoplasm, as revealed by freeze-etching of the squid giant nerve fiber, in relation to actin, tubulin and myosin components. *Biol. Bull.* **147**:491. (Abstr.).
30. METUZALS, J., and I. TASAKI. 1976. Scanning electron microscopy of filamentous network on the cytoplasmic face of the axolemma. *J. Cell Biol.* **70** (2, Pt. 2):39*a*. (Abstr.).
31. MOMMAERTS, W. F. H. M., and R. G. PARRISH. 1951. Studies on myosin. I. Preparation and criteria of purity. *J. Biol. Chem.* **188**:545–552.
32. MOOSEKER, M. S., and L. G. TILNEY. 1975. Orga-

nization of an actin filament-membrane complex. Filament polarity and membrane attachment in the microvilli of intestinal epithelial cells. *J. Cell Biol.* **67**:725–743.

33. NEEDHAM, J. 1936. Order and Life. Yale University Press, New Haven.
34. NICOLSON, G. L. 1976. Transmembrane control of the receptors on normal and tumor cells. I. Cytoplasmic influence over cell surface components. *Biochim. Biophys. Acta.* **457**:57–108.
35. NICOLSON, G. L., V. T. MARCHESI, and S. J. SINGER. 1971. The localization of spectrin on the inner surface of human red blood cell membranes by ferritin-conjugated antibodies. *J. Cell Biol.* **51**:265–272.
36. ORREGO, F. 1971. Protein degradation in squid giant axons. *J. Neurochem.* **18**:2249–2254.
37. PAINTER, R. G., M. SHEETZ, and S. J. SINGER. 1975. Detection and ultrastructural localization of human smooth muscle myosin-like molecules in human non-muscle cells by specific antibodies. *Proc. Natl. Acad. Sci. U. S. A.* **72**:1359–1363.
38. POLLARD, T. D., E. SHELTON, R. R. WEIHING, and E. D. KORN. 1970. Ultrastructural characterization of F-actin isolated from *Acanthamoeba castellanii* and identification of cytoplasmic filaments as F-actin by reaction with rabbit heavy meromyosin. *J. Mol. Biol.* **50**:91–97.
39. POLLARD, Th. D., and E. D. KORN. 1973. Electron microscopic identification of actin associated with isolated amoeba plasma membranes. *J. Biol. Chem.* **248**:448–450.
40. POLLARD, T. D., and R. R. WEIHING. 1974. Actin and myosin and cell movement. *CRC Crit. Rev. Biochem.* **2**:1–65.
41. PORTER, K., D. PRESCOTT, and J. FRYE. 1973. Changes in surface morphology of Chinese hamster ovary cells during the cell cycle. *J. Cell Biol.* **57**:815–836.
42. REYNOLDS, E. S. 1963. The use of lead citrate at high pH as an electron-opaque stain in electron microscopy. *J. Cell Biol.* **17**:208–212.
43. REYNONDS, J. A., and H. TRAYER. 1971. Solubility of membrane proteins in aqueous media. *J. Biol. Chem.* **246**:7337–7342.
44. RÖHLICH, P. 1975. Membrane-associated actin filaments in the cortical cytoplasm of the rat mast cell. *Exp. Cell Res.* **93**:293–298.
45. SATO, H., I. TASAKI, E. CARBONE, and M. HALLETT. 1973. Changes in axon birefringence associated with excitation: Implications for the structure of the axon membrane. *J. Mechanochem. Cell Motility.* **2**:209–217.
46. SCHEKMAN, R., and S. J. SINGER. 1976. Clustering and endocytosis of membrane receptors can be induced in mature erythrocytes of neonatal but not adult humans. *Proc. Natl. Acad. Sci. U. S. A.* **73**:4075–4079.
47. SCOTT, R. E. 1976. Plasma membrane vesiculation: a new technique for isolation of plasma membranes. *Science (Wash. D. C.).* **194**:743–745.
48. SEE, Y. P., and J. METUZALS. 1976. Purification and characterization of squid brain myosin. *J. Biol. Chem.* **251**:7682–7689.
49. SHEETZ, M. P., and S. M. HOM. 1976. Actin binding to lipids. *J. Cell Biol.* **70** (2, Pt. 2):305*a*. (Abstr.).
50. SINGER, S. J. 1974. The molecular organization of membranes. *Annu. Rev. Biochem.* **43**:805–833.
51. SINGER, S. J. 1974. Molecular biology of cellular membranes with applications to immunology. *Adv. Immunol.* **19**:1–66.
52. SINGER, S. J. 1975. Membrane fluidity and cellular functions. *In* Control Mechanisms in Development. R. H. Meints and E. Davier, editors. Plenum Press, New York. 181–192.
53. SPUDICH, J. A. 1974. Biochemical and structural studies of actomyosin-like proteins from non-muscle cells. II. Purification, properties, and membrane association of actin from amoebae of *Dictyostelium discoideum*. *J. Biol. Chem.* **249**:6013–6020.
54. SPUDICH, J. A., and S. WATT. 1971. The regulation of rabbit skeletal muscle contraction. I. Biochemical studies of the interaction of the tropomyosin-troponin complex with actin and the proteolytic fragments of myosin. *J. Biol. Chem.* **246**:4866–4871.
55. STECK, Th. L. 1974. The organization of proteins in the human red blood cell membrane. *J. Cell Biol.* **62**:1–19.
56. STECK, Th. L., R. S. WEINSTEIN, J. H. STRAUS, and D. F. H. WALLACH. 1970. Inside-out red cell membrane vesicles: preparation and purification. Science (*Wash. D. C.*). **168**:255–257.
57. SZENT-GYÖRGYI, A. 1945. Studies on muscle. Part VI. The preparation and crystallization of myosin. *Acta Physiol. Scand.* **8** (*Suppl.* 25):82–95.
58. TAKENAKA, T., R. HIRAKOW, and S. YAMAGISHI. 1968. Ultrastructural examination of the squid giant axons perfused intracellularly with protease. *J. Ultrastruct. Res.* **25**:408–416.
59. TASAKI, I. 1968. Nerve excitation. A macromolecular approach. Charles C. Thomas, Publisher. Springfield, Ill.
60. TASAKI, I., A. WATANABE, and M. HALLETT. 1971. Properties of squid axon membrane as revealed by a hydrophobic probe, 2-*p*-toluidinylnaphthalene-6-sulfonate. *Proc. Natl. Acad. Sci. U. S. A.* **68**:938–941.
61. VACQUIER, V. D. 1975. The isolation of intact cortical granules from sea urchin eggs: calcium ions trigger granule discharge *Dev. Biol.* **43**:62–74.
62. VIAL, J. D., and J. GARRIDO. 1976. Actin-like filaments and membrane rearrangement in oxyntic cells. *Proc. Natl. Acad. Sci. U. S. A.* **73**:4032–4036.
63. VILLEGAS, J. 1972. Axon-Schwann cell interaction in the squid nerve fibre. *J. Physiol. (Lond.).* **225**:275–296.

64. WEBER, K., and M. OSBORN. 1969. The reliability of molecular weight determinations by dodecyl sulfate-polyacrylamide gel electrophoresis. *J. Biol. Chem.* **244:**4406–4412.
65. WICKUS, G., E. GRUENSTEIN, Ph. W. ROBBINS, and A. RICH. 1975. Decrease in membrane-associated actin of fibroblasts after transformation by Rous sarcoma virus. *Proc. Natl. Acad. Sci. U. S. A.* **72:**746–749.
66. WOODRUM, D. T., S. A. RICH, and T. D. POLLARD. 1975. Evidence for biased bidirectional polymerization of actin filaments using heavy meromyosin prepared by an improved method. *J. Cell Biol.* **67:**231–237.
67. YAMADA, K. M., B. S. SPOONER, and N. K. WESSELS. 1971. Ultrastructure and function of growth cones and axons of cultured nerve cells. *J. Cell Biol.* **49:**614–635.